

GR-81-9

HYDRAULIC MODEL STUDY OF DAULE-PERIPA SPILLWAY AND OUTLET WORKS

June 1981

Engineering and Research Center



*U.S. Department of the Interior
Bureau of Reclamation
Division of Research
Hydraulics Branch*

TECHNICAL REPORT STANDARD TITLE PAGE

1. REPORT NO. GR-81-9		2. GOVERNMENT ACCESSION NO.		3. RECIPIENT'S CATALOG NO.	
4. TITLE AND SUBTITLE Hydraulic Model Study of Daule-Peripa Spillway and Outlet Works				5. REPORT DATE June 1981	
				6. PERFORMING ORGANIZATION CODE	
7. AUTHOR(S) Kathleen L. Houston				8. PERFORMING ORGANIZATION REPORT NO. GR-81-9	
9. PERFORMING ORGANIZATION NAME AND ADDRESS Bureau of Reclamation Engineering and Research Center Denver, Colorado 80225				10. WORK UNIT NO.	
				11. CONTRACT OR GRANT NO.	
12. SPONSORING AGENCY NAME AND ADDRESS Daule-Peripa Multiple Purpose Project Ecuador, South America				13. TYPE OF REPORT AND PERIOD COVERED	
				14. SPONSORING AGENCY CODE DIBR	
15. SUPPLEMENTARY NOTES					
Editor: JMT					
16. ABSTRACT					
<p>Two hydraulic models were built and studied to verify the original design of the Daule-Peripa spillway and outlet works to be constructed on the Daule River in Ecuador. The 1:80-scale spillway model included the approach channel, spillway, outlet works, powerplant, and downstream river channel. The model showed that excavation was not necessary in the spillway approach channel. A discharge curve and gate opening combinations were derived from the model. The flow over the crest was satisfactory with the piers shortened; however, it impinged upon the gate trunnion pins at higher discharges. On the spillway chute, all offsets greater than 3 mm should be ground to a 1:10 chamfer. The stilling basin walls were over-topped for discharges greater than 2300 m³/s; however, pressures indicated that they would remain stable. The velocities downstream of the stilling basin were within the design range; however, the riverbed eroded for about 24 m downstream of the apron. The 1:50.65-scale outlet works model included two 9-m-diameter concrete-lined tunnels with intakes for either diversion flow or for flow through the penstock and permanent outlet works. The model provided discharge information for the uncontrolled diversion flow and the gated permanent outlet works. Flow through the tunnel bends and velocities downstream of the stilling basins were satisfactory. No erosion occurred downstream of the outlet works or the powerplant. The penstock intake with the trashrack installed passed all discharges without vortices being formed.</p>					
17. KEY WORDS AND DOCUMENT ANALYSIS					
<p>a. DESCRIPTORS-- / hydraulics/ hydraulic models/ spillway approach/ radial gates/ spillway/ outlet works tunnel/ velocity measurements/ erosion/ cavitation potential/ diversion discharge/ penstock bellmouth intake/ vortices/ pressures</p> <p>b. IDENTIFIERS-- / Daule-Peripa Dam, Ecuador; CEDEGE (Comision de Estudios Para el Desarrollo de la Cuenca del Rio Guayos)</p> <p>c. COSATI Field/Group 13B COWRR: 1313.1 SRIM: 50B</p>					
18. DISTRIBUTION STATEMENT				19. SECURITY CLASS (THIS REPORT) UNCLASSIFIED	
				21. NO. OF PAGES 83	
				20. SECURITY CLASS (THIS PAGE) UNCLASSIFIED	
				22. PRICE	

GR-81-9

**HYDRAULIC
MODEL STUDY OF
DAULE - PERIPA
SPILLWAY AND
OUTLET WORKS**

by
Kathleen L. Houston
for Daule-Peripa Project
Ecuador, South America

Hydraulics Branch
Division of Research
Engineering and Research Center
Denver, Colorado

June 1981



ACKNOWLEDGMENTS

I would like to express my appreciation to Dr. Jack Hilf and Mr. Harold Arthur, consulting engineers in Denver, Colorado. Their roles as coordinators between the TAMS (Tippets-Abbett-McCarthy-Stratton) designers, the project directors in Ecuador, and the Bureau of Reclamation hydraulics laboratory personnel were invaluable. The visits by Mr. Herbert Witte, the TAMS consultant in Ecuador, and Mr. Marco Dominguez, the project director, always provided an excellent opportunity for meaningful discussions and clarifications.

As the Nation's principal conservation agency, the Department of the Interior has responsibility for most of our nationally owned public lands and natural resources. This includes fostering the wisest use of our land and water resources, protecting our fish and wildlife, preserving the environmental and cultural values of our national parks and historical places, and providing for the enjoyment of life through outdoor recreation. The Department assesses our energy and mineral resources and works to assure that their development is in the best interests of all our people. The Department also has a major responsibility for American Indian reservation communities and for people who live in Island Territories under U.S. administration.

In May of 1981, the Secretary of the Interior approved changing the Water and Power Resources Service back to its former name, the Bureau of Reclamation.

CONTENTS

	Page
Acknowledgments	ii
Introduction	1
Results	1
The models	5
Similitude and test discharges	7
The spillway model	8
The approach channel	8
Flow impingement on gate trunnions	8
Pier modification	9
Gate opening combinations	9
Crest shape	11
Water surface profiles	11
Cavitation potential	12
Pressures on the stilling basin walls	12
Riverbed stabilization	14
Velocity profiles	14
Erosion tests	14
The outlet works model	15
Diversion condition	15
Modified entrance—tunnel No. 1	16
Permanent outlet works—tunnel No. 1	16
Velocities and erosion downstream of the stilling basins and powerplant	17
Powerplant intake	17
Trashrack structure	18

TABLES

Table	Page
1 Water manometer pressure data for the right wall of the spillway stilling basin, spillway $Q = 1000 \text{ m}^3/\text{s}$, spillway-powerplant-outlet works $Q = 1650 \text{ m}^3/\text{s}$	19
2 Water manometer pressure data for the right wall of the spillway stilling basin, spillway $Q = 1500 \text{ m}^3/\text{s}$, spillway-powerplant-outlet works $Q = 2150 \text{ m}^3/\text{s}$	19

CONTENTS—Continued

Table	Page	
3	Water manometer pressure data for the right wall of the spillway stilling basin, spillway $Q = 2000 \text{ m}^3/\text{s}$, spillway-powerplant-outlet works $Q = 2650 \text{ m}^3/\text{s}$	20
4	Water manometer pressure data for the right wall of the spillway stilling basin, spillway $Q = 2500 \text{ m}^3/\text{s}$, spillway-powerplant-outlet works $Q = 3150 \text{ m}^3/\text{s}$	20
5	Water manometer pressure data for the right wall of the spillway stilling basin, spillway $Q = 3000 \text{ m}^3/\text{s}$, spillway-powerplant-outlet works $Q = 3650 \text{ m}^3/\text{s}$	21
6	Transducer pressure data for the right wall of the spillway stilling basin spillway $Q = 3600 \text{ m}^3/\text{s}$, spillway-powerplant-outlet works $Q = 4250 \text{ m}^3/\text{s}$	21
7	Transducer pressure data for the right wall of the spillway stilling basin spillway $Q = 1000 \text{ m}^3/\text{s}$, spillway-powerplant-outlet works $Q = 1650 \text{ m}^3/\text{s}$	22
8	Transducer pressure data for the right wall of the spillway stilling basin spillway $Q = 1500 \text{ m}^3/\text{s}$, spillway-powerplant-outlet works $Q = 2150 \text{ m}^3/\text{s}$	22
9	Transducer pressure data for the right wall of the spillway stilling basin spillway $Q = 2000 \text{ m}^3/\text{s}$, spillway-powerplant-outlet works $Q = 2650 \text{ m}^3/\text{s}$	23
10	Transducer pressure data for the right wall of the spillway stilling basin spillway $Q = 2500 \text{ m}^3/\text{s}$, spillway-powerplant-outlet works $Q = 2900 \text{ m}^3/\text{s}$	23
11	Transducer pressure data for the right wall of the spillway stilling basin spillway $Q = 3000 \text{ m}^3/\text{s}$, spillway-powerplant-outlet works $Q = 3400 \text{ m}^3/\text{s}$	24
12	Transducer pressure data for the right wall of the spillway stilling basin spillway $Q = 3600 \text{ m}^3/\text{s}$, spillway-powerplant-outlet works $Q = 4000 \text{ m}^3/\text{s}$	24
13	Water manometer pressure data for the outlet works tunnel bend	25

FIGURES

Figure	Page	
1	General project plan	27
2	Profile of permanent outlet works structure, tunnel No. 1	29
3	Profile of powerplant penstock, tunnel No. 2	31

CONTENTS—Continued

Figure		Page
4	Tailwater curve	33
5	Overall view of the 1:50.62 outlet works model in foreground; 1:80 spillway model in background	34
6	Spillway plan and section showing proposed excavation of approach channel	35
7	Approach channel with proposed excavation filled in, located about 500 m upstream of spillway crest	37
8	Right side of approach channel adjacent to crest, with original topography restored	37
9	Flow pattern adjacent to crest: $Q = 2000 \text{ m}^3/\text{s}$ for the improved channel	38
10	Impingement of flow on the gate trunnions: $Q = 2600 \text{ m}^3/\text{s}$	38
11	Submergence of all trunnions: $Q = 3600 \text{ m}^3/\text{s}$	39
12	Piers streamlined and shortened to STA 1 + 20.5	39
13	Piers shortened to trunnion supports	40
14	Flow with recommended gate openings for $Q = 1000 \text{ m}^3/\text{s}$	40
15	Flow with recommended gate openings for $Q = 2000 \text{ m}^3/\text{s}$	41
16	Discharge curve for gate controlled and uncontrolled crest	42
17	Water surface profiles for the left wall of the spillway chute	43
18	Water surface profiles for the right wall of the spillway chute	44
19	Computer printout for cavitation analysis at $Q = 200 \text{ m}^3/\text{s}$	45
20	Computer printout for cavitation analysis at $Q = 500 \text{ m}^3/\text{s}$	47
21	Computer printout for cavitation analysis at $Q = 1000 \text{ m}^3/\text{s}$	49
22	Computer printout for cavitation analysis at $Q = 2000 \text{ m}^3/\text{s}$	51
23	Spillway stilling basin operation for $Q = 1000 \text{ m}^3/\text{s}$ and tailwater EL 25	53
24	Spillway stilling basin operation for $Q = 2000 \text{ m}^3/\text{s}$ and tailwater EL 33.4	53
25	Spillway stilling basin operation for $Q = 3600 \text{ m}^3/\text{s}$ and tailwater EL 41.5	54
26	Piezometer locations along the right wall of the spillway stilling basin	54
27	Stabilized riverbed for spillway model	55
28	Graphical representation of the velocities downstream of the spillway stilling basin, $Q = 1000 \text{ m}^3/\text{s}$, tailwater EL 27	56
29	Graphical representation of the velocities downstream of the spillway stilling basin, $Q = 1500 \text{ m}^3/\text{s}$, tailwater EL 30.4	57
30	Graphical representation of the velocities downstream of the spillway stilling basin, $Q = 2000 \text{ m}^3/\text{s}$, tailwater EL 33.4	58
31	Graphical representation of the velocities downstream of the spillway stilling basin, $Q = 2500 \text{ m}^3/\text{s}$, tailwater EL 36.2	59
32	Graphical representation of the velocities downstream of the spillway stilling basin, $Q = 3000 \text{ m}^3/\text{s}$, tailwater EL 38.7	60
33	Graphical representation of the velocities downstream of the spillway stilling basin, $Q = 3600 \text{ m}^3/\text{s}$, tailwater EL 41	61

CONTENTS—Continued

Figure	Page
34 Erosion at the toe of the spillway apron and along the left riverbank	62
35 Deposition of eroded material downstream of the spillway sill	62
36 Eroded material collected behind the left spillway training wall	63
37 Eroded material deposited downstream of the spillway in the river channel at STA 1 + 684.0	63
38 Diversion intake structures, reservoir EL 30, $Q = 593.6 \text{ m}^3/\text{s}$	64
39 Diversion intake structures, reservoir EL 40, $Q = 1472.7 \text{ m}^3/\text{s}$	64
40 Diversion intake structures, reservoir EL 53, $Q = 2007.9 \text{ m}^3/\text{s}$	65
41 Diversion stilling basin operation, reservoir EL 30, $Q = 593.6 \text{ m}^3/\text{s}$, tailwater EL 23.8	65
42 Diversion stilling basin operation, reservoir EL 40, $Q = 1472.7 \text{ m}^3/\text{s}$, tailwater EL 30.3	66
43 Diversion stilling basin operation, reservoir EL 53, $Q = 2007.9 \text{ m}^3/\text{s}$, tailwater EL 33.6	66
44 Diversion discharge curve (both tunnels operating)	67
45 Modified selective withdrawal tower for the permanent outlet works	68
46 Tunnel bend with reservoir EL 85, $Q = 422 \text{ m}^3/\text{s}$	69
47 Oscillating flow downstream of the tunnel bend with reservoir EL 85, $Q = 422 \text{ m}^3/\text{s}$	69
48 Stilling basin operation for $Q = 422 \text{ m}^3/\text{s}$ and reservoir EL 85	70
49 Stabilized outlet works model riverbed	70
50 Graphical representation of the velocities downstream of the outlet works stilling basin, $Q = 422 \text{ m}^3/\text{s}$, tailwater EL 22.5	71
51 Graphical representation of the velocities downstream of the outlet works stilling basin, $Q = 672 \text{ m}^3/\text{s}$, tailwater EL 24.6	72
52 Graphical representation of the velocities present downstream for powerplant operation only, $Q = 250 \text{ m}^3/\text{s}$, tailwater EL 20.7	73
53 Graphical representation of the velocities present downstream for powerplant and outlet works operation, $Q = 672 \text{ m}^3/\text{s}$, tailwater EL 24.6	73
54 Bellmouth intake structure	74
55 Vortex at the bellmouth intake for reservoir EL 70 without the trashrack	74
56 Vortex at the bellmouth intake for reservoir EL 75 without the trashrack	75
57 Vortex at the bellmouth intake for reservoir EL 80 without the trashrack	75
58 Vortex at the bellmouth intake for reservoir EL 85 without the trashrack	76
59 No vortex formed at reservoir EL 60, $Q = 100 \text{ m}^3/\text{s}$, with the trashrack	76
60 No vortex formed at reservoir EL 75, $Q = 250 \text{ m}^3/\text{s}$, with the trashrack	77
61 No vortex formed at reservoir EL 85, $Q = 250 \text{ m}^3/\text{s}$, with the trashrack	77

INTRODUCTION

The Daule River in Ecuador is the main waterway along the eastern slope of the Andes Mountains. The river basin extends from high in the mountains to the mouth of the river near Guayaquil, where the waters enter the Pacific Ocean.

The Daule-Peripa Dam will be located on the Daule River approximately 160 km upstream of Guayaquil, Ecuador. The dam is being constructed by the CEDEGE (Comision de Estudios para el Desarrollo de la Cuenca del Rio Guayas) and financed by the Ecuadorian Government. The designer of the project was TAMS (Tippetts-Abbett-McCarthy-Stratton), of New York and Guayaquil. The Bureau of Reclamation was contacted by the CEDEGE consultants to perform a model study of the Daule-Peripa Dam, spillway, and outlet works.

The Daule-Peripa Project consists of an earthfill dam with a spillway, outlet works, and powerplant. Figure 1 shows the location of the spillway, outlet works, and powerplant. The dam will be 90 m high, with water flowing over a radial gate-controlled crest atop a 59-m-wide, 387-m-long spillway chute, and discharging into a 124-m-long stilling basin. Two 9-m-diameter concrete-lined tunnels located to the right of the spillway will be used to divert the river during construction. Intakes for the permanent outlet works and powerplant will be added to the tunnels after diversion is complete (figs. 2 and 3).

The project's main objectives will be to provide flood control, irrigation, and hydro-power, and to maintain the vital transportation route of the river.

RESULTS

The results of the spillway tests (1:80 scale model) are:

- A. The proposed excavation in the approach channel approximately 500 m upstream of the spillway crest is not necessary. The natural topography in this area did not cause any disturbances in the approach flow throughout the discharge range studied.

B. The excavated area upstream of the dam embankment adjacent to the right side of the spillway caused turbulence, undesirable swirling action, and unequal flow distribution into the right spillway bay. When this area was restored to closely approximate the natural topography, the turbulence was eliminated and the flow distribution improved.

C. Flow impinged on the right trunnion pin in the right bay when the discharge reached 2600 m³/s at reservoir EL 85.49. This is due to a slightly larger quantity of flow through this bay. However, as the discharge increases, the trunnions in all bays eventually become submerged.

D. The spillway piers were shortened to STA. 1+14.0, just downstream of the trunnion supports, with no adverse effect on the flow distribution. The ends of the piers were not streamlined.

E. The spillway crest has a discharge coefficient of 2.000 at the maximum discharge head. The spillway will pass a free-flow discharge of 2300 m³/s at reservoir EL 85 and a discharge of 3750 m³/s at reservoir EL 88.

F. A comparative analysis of the Daule-Peripa crest shape with similar crests studied in previous laboratory investigations indicated that subatmospheric pressures on the crest surface would not exist.

G. For two-gate operation and discharges up to 1000 m³/s, the best flow patterns along the chute occurred with the center gate closed. The other gate combinations—the left or right gate closed—also produced satisfactory flow distribution. If it is necessary under two-gate operation to increase the discharge to 2000 m³/s, only the right gate should be closed; when either of the other gates are closed, the chute sidewalls are overtopped.

Total discharge, Q (m ³ /s)	Spillway gates		
	Left	Center	Right
1000	Open	Closed	Open
1000	Closed	Open	Open
1000	Open	Open	Closed
2000	Open	Open	Closed

H. Using the tailwater curve shown in figure 4, the stilling basin formed an efficient hydraulic jump with adequate energy dissipation for discharges up to 2300 m³/s. Above this discharge and tailwater EL 35, the stilling basin was adequate; however, weir flow occurred over the training walls of the stilling basin. The weir flow over the basin training walls did not produce subatmospheric pressures or pressure fluctuations great enough to endanger the stability of the walls. The effects of the weir flow should be minimal, provided the walls were designed for full hydrostatic pressure.

I. The velocities downstream of the spillway stilling basin were all below the design value of 5.0 m/s, with the exception of three instantaneous values (about 6.4 m/s) at a discharge of 3600 m³/s. At the end of the stilling basin apron, the velocities were lower along the centerline and increased on either side of the centerline.

J. The channel below the spillway was formed using a sand-cement mixture to represent a weak sandstone material. Erosion occurred at the left toe of the spillway apron and continued for 12 m downstream causing minor undermining of the left bank in this area. The undermining of the bank was accompanied by wave action at the water surface which also contributed to the bank erosion. The eroded area extended to approximately 24.4 m downstream of the apron.

The eroded material was deposited in three places. For discharges up to 1500 m³/s, the eroded material was alternately drawn up onto the apron where it collected immediately downstream of the end sill and eventually moved out. Material eroded by the higher discharges remained on the apron. The eroded material formed a 2- to 3-m-high bar across the river channel at STA 1+684.0 at all discharges. When the tailwater elevation was above 34 m, eroded material was deposited behind the left spillway training wall from STA 1+434.5 to STA 1+448.67.

K. Cavitation potential along the spillway chute was analyzed using a computer program. Extreme care should be used on the surface finish from STA 1+40.0 to STA 1+60.0 and on the vertical curve transition from the chute to the stilling basin. Offsets greater than 3 mm high should be ground to a 1:10 chamfer. In the remainder of the chute, the program indicated offsets of 10 mm were permissible before incipient cavitation occurred.

The results of outlet works tests (1:50.62 scale model) are:

A. The uncontrolled diversion flow for both tunnels was studied. At reservoir EL 30, the discharge capacity was 593.6 m³/s; neither tunnel intake was submerged. At reservoir EL 40 and 53, the discharge capacity was 1472.7 and 2007.9 m³/s, respectively; the intakes were submerged and both tunnels flowed full. At reservoir EL 40, vortices formed over the entrances of both tunnels. The vortex over tunnel No. 1 was very persistent, with the vortex at tunnel No. 2 smaller and weaker. No vortex formed over the intake of either tunnel with the reservoir at EL 53; however, a dimple formed on the water surface above tunnel No. 1 indicating a vortex may form in the prototype.

B. The permanent gate-controlled outlet works (tunnel No. 1) at one-half, three-fourths, and fully open, without powerplant operation, produced discharges of 190, 310, and 422 m³/s, respectively, at reservoir EL 85. With powerplant in operation, the discharges were 190, 297, and 399 m³/s, respectively. The prototype discharges should

be slightly higher because the model intake did not include the selective withdrawal tower or the bellmouth entrances.

C. The tunnel bends, under all operating conditions, produced no adverse flow distribution or subatmospheric pressures.

D. The stilling basins provided adequate energy dissipation for all discharges as indicated by low velocities and the absence of erosion in the downstream channel.

E. The penstock bellmouth intake (tunnel No. 2) was tested at a discharge of 250 m³/s both with and without the trashrack structure. Without the trashrack structure, vortices were larger and more consistent at the lower elevations of 60, 65, and 70 m. With the trashrack structure in place over the bellmouth entrance, the vortices were present only at reservoir EL 60 and 65. When the water surface was above the top of the trashrack structure, the vortices were suppressed. At a discharge of 100 m³/s, no vortices were present at the reservoir elevations tested.

F. The powerplant operating alone or simultaneously with the outlet works caused no erosion problems in the riverbed downstream of the structure.

THE MODELS

The study utilized two separate models. The 1:80 scale spillway model and the 1:50.62 scale outlet works model are shown on figure 5.

The spillway headbox included 650 m of upstream reservoir area; the tailbox included 1100 m downstream from the dam. The reservoir topography was made using concrete; the downstream channel and topography formed using a sand-cement mixture which approximated the erodibility of the prototype area. The erodible topography was formed using templates of the river cross sections. The hydraulic structures included the spillway

crest with piers and gates, the spillway chute and stilling basin, the outlet works stilling basins, and the powerplant.

The control crest was 59 m wide with three 17-m bays separated by 4-m-wide piers. The crest and piers were constructed of high-density polyurethane foam.

The three radial control gates were made of metal with rubber seals. The spillway chute sloped (0.5375 percent) to a vertical curve, which formed the transition to the stilling basin. The trapezoidal cross section of the stilling basin had 10:1 side walls and was 124 m long. The basin floor had a sloping section at the base of the vertical curve ending on the flat bottom of the basin with a 6.5-m-high sill located at STA 1 + 498.0. The apron and sidewalls extended an additional 55 m downstream. Both the outlet works stilling basins and the powerplant were included. The stilling basins were included downstream of the transitions to the sills, with 33.0-m-long aprons downstream of the sills. The powerplant included the tailrace structure. These structures were all constructed of plywood. Water was supplied to the permanent outlet works and the powerplant through two pipes connected to the headbox reservoir.

The 1:50.62 scale model of the outlet works consisted of a separate headbox and tailbox joined by the outlet works and powerplant tunnels. The headbox included 160 m of upstream reservoir topography formed using concrete. The hydraulic structures in the headbox included both diversion intakes. These intakes were subsequently replaced with a modified selective withdrawal tower intake for the permanent outlet works of tunnel No. 1 and a bellmouth intake for powerplant penstock tunnel No. 2. These intake structures were formed of acrylic plastic and high-density polyurethane with the bellmouth portion of the powerplant intake constructed of sheet metal. The 9.0-m outlet tunnels were both constructed of acrylic plastic pipe with the radius of curvature of the pipe bends equal to 180 m. A subsequent modification to the radius of curvature of the powerplant tunnel was not tested as it was not received until after completion of construction and the radius had been increased, lessening the severity of the bend. The tunnels entered the tailbox at their respective portal stations. The transition structures from both

tunnels to trapezoidal stilling basins were formed with sheet metal and the warped surfaces shaped using concrete. The tailbox included the outlet works stilling basins, with a short length of the spillway apron downstream of the stilling basin to the left, and the powerplant to the right. The powerplant was oriented at an angle of 30° with respect to STA 1 + 550.0 of tunnel No. 2 (fig. 1). The riverbed in this model was also constructed of a sand-cement mixture to represent the weak sandstone material.

The tailwater in both models was set by using wheel-operated tailgates. Water was supplied to both models by the laboratory venturi system.

Similitude and Test Discharges

Both models were constructed to linear scales determined by Froude relationships. The model variables were computed as follows:

$$\text{Model discharge } (Q_m) = \frac{1}{(N^{2.5})} Q_p$$

$$\text{Model velocity } (V_m) = \frac{1}{(N^{0.5})} V_p$$

where: $N = 80$ for the spillway model
 $N = 50.62$ for the outlet works model

For instance, a spillway prototype discharge, Q_p of 2000 m^3/s , produced a model discharge, Q_m of 0.03494 m^3/s , computed as follows:

$$Q_m = \frac{1}{(80)^{2.5}}(2000) = 0.03494 \text{ m}^3/\text{s}$$

For the spillway, test discharges were 1000, 1500, and 2000 m^3/s under gate control with a reservoir elevation of 85 m. For the test discharges of 2500, 3000, and 3600 m^3/s (without gate control); the reservoir elevations were 85.5, 86.5, and 87.75 m, respectively.

The erosion tests were run on a qualitative basis only. For the discharges tested, general areas of erosion were observed; however, the quantities cannot be accurately determined from the model.

THE SPILLWAY MODEL

The Approach Channel

Approach channel conditions were tested for two areas of proposed excavation, one about 500 m upstream of the crest and the other adjacent to the crest on the right side. The proposed excavations are shown on figure 6. Observations of the approach channel flow in the model indicated that the excavation located 500 m upstream of the crest might not be necessary. Therefore, pea gravel was used to simulate the original topography, as shown on figure 7. This area was investigated using colored dye and confetti to observe the flow patterns. These tests showed that the narrower opening would not constrict the flow.

The proposed excavation immediately adjacent to the crest on the right side of the approach channel produced an unsatisfactory flow distribution. The ridge at EL 81.5 that remained when the channel was formed caused high velocity lateral flow to occur in the area. This was observed by spreading confetti and dye over the channel in that area. This area of the approach channel was restored to its natural topography (fig. 8) and the flow distribution greatly improved through the spillway bays. Figure 9 shows the improvement in the lateral flow adjacent to the crest for the restored original topography at a discharge of 2000 m³/s.

Flow Impingement on Gate Trunnions

Flow impinged slightly upon the right trunnion of the right spillway bay at a discharge of 2600 m³/s and reservoir EL 85.65, as shown on figure 10. Impingement increased as the

flow increased with submergence of all trunnions in all bays occurring at 3600 m³/s (fig. 11). The impingement caused slight splashing to occur on the right crest abutment downstream of the dam, which could lead to erosion behind the right training wall.

Pier Modification

The downstream edges of the spillway crest piers were gradually moved upstream from STA 1+40.0. The piers' downstream edges were first streamlined and shortened to STA 1+20.5 as shown on figure 12. The piers were then tested with the downstream edges not streamlined. A fin was formed downstream from the end of the pier; however, it did not interfere with the flow distribution. The piers' downstream edges were then terminated at STA 1+14.0 downstream of the trunnions, as shown on figure 13. Gate openings were tested with each pier modification with no adverse effects indicated. The square-end pier was used because it did not disturb the flow on the spillway chute and should be easier to construct. The savings in concrete with the downstream end of the piers shortened from STA 1+40.0 to STA 1+14.0 would be approximately 912 m³.

Gate Opening Combinations

Uniform gate openings provide the most uniform flow distribution and should be used whenever possible.

The shorter spillway piers allowed the flow through each bay to merge prior to reaching the base of the crest, thus making overtopping of the training walls more likely during nonuniform gate operation. Spillway gate opening combinations were tested to determine the best alternative available for nonuniform gate operation. Nonuniform gate operation, specifically one gate closed as would occur during maintenance of a gate or malfunction of a hoist, was tested at discharges of 1000 and 2000 m³/s. The openings were based upon visual observations of the flow and velocity distribution. Immediately eliminated were those gate openings which caused overtopping of the training walls or extremely uneven flow distribution.

With the piers shortened to STA 1+14.0 and a discharge of 1000 m³/s, the best two-gate operation occurred with the middle gate fully closed. This produced the most uniform flow distribution on the chute as shown on figure 14. The other combinations, left or right gate closed, also produced satisfactory flow distribution. If it is necessary to increase the discharge to 2000 m³/s, the right gate should be closed, and all flow routed through the other two gates (fig. 15).

At 2000 m³/s (with the middle gate closed), overtopping of the training walls occurred on both sides of the chute at about STA 1+235. With the left gate closed, the flow was very close to overtopping the left side of the chute at about STA 1+222. The recommended sequencing arrangements are shown below:

Total discharge, Q (m ³ /s)	Spillway gates		
	Left	Center	Right
1000	Open	Closed	Open
1000	Closed	Open	Open
1000	Open	Open	Closed
2000	Open	Open	Closed

The sequencing was only done up to reservoir EL 85 and at a discharge of 2000 m³/s. Discharges greater than this require uncontrolled flow. The most uniform flow distribution for three-gate unequal gate operation was:

Total discharge, Q (m ³ /s)	Spillway gates		
	Left (m ³ /s)	Center (m ³ /s)	Right (m ³ /s)
1000	500	0	500
1500	666.67	333.33	500
2000	833.33	500	666.67

Crest Shape

The spillway crest shape was checked theoretically for subatmospheric pressures which may lead to flow instability or cavitation. Using Engineering Monograph No. 9,* the crest shape was compared to other crest shapes with known pressure profiles and discharge coefficients. The procedure consisted of dividing all the dimensions by the total head and plotting these dimensionless values on an X-Y plane. The shape compared closely with the Canyon Ferry Dam and Hirakud Dam shapes, both of which had a positive pressure profile throughout the crest shape. The crest shape has a discharge coefficient of 2.000 as indicated by the plot of reservoir elevation versus discharge coefficient on figure 16.

Three 17.0- by 11.90-m radial gates were used to control the flow over the crest up to reservoir EL 85. The discharge curves for controlled and uncontrolled flow are shown on figure 16.

Water Surface Profiles

Water surface profiles were measured along the length of the chute from the base of the crest at STA 1+40.0 to the beginning of the transition at STA 1+373.0. Data were taken every 50 m for each test discharge along both the right and left walls of the chute. The profiles are shown graphically on figures 17 and 18. The water surface profiles follow the typical S3 profile with the actual and normal depths less than the critical depth, indicating supercritical flow. The flow is contained within the chute walls except for the 3600-m³/s discharge which overtopped the left wall at approximately STA 1+212.0.

* Bradley, J. N., "Discharge Coefficients for Irregular Overfall Spillways," Engineering Monograph No. 9, U.S. Department of the Interior, Bureau of Reclamation, Denver, Colorado, March 1952.

Cavitation Potential

The cavitation potential along the spillway chute between STAS 1+40.0 and 1+373.0 was analyzed using a computer program. The cavitation analysis was based upon presently available information which includes boundary layer effects.* The computer program has been undergoing some modification and verification as data became available from performance of existing prototype structures. Discharges of 200, 500, 1000, and 2000 m³/s were investigated. Initially the program had predicted incipient cavitation between STAS 1+40.0 and 1+100.0 and also at STA 1+373.0. Aeration slots were recommended at STAS 1+40.0 and 1+373.0; however, the program has since indicated that the chute will operate satisfactorily with little or no cavitation damage without the aeration slots. Care must still be taken with the surface finish between STAS 1+40.0 and 1+60.0, and also on the vertical curve transition from the chute to the stilling basin. As shown on figure 29, the hydraulic jump is contained within the stilling basin below STA 1+373.0 for the maximum discharge of 3600 m³/s. All surface irregularities in these areas greater than 3 mm high should be ground to a 1:10 chamfer. In the remainder of the chute, irregularities greater than 10 mm should be ground to a 1:5 chamfer. The computer printouts of the cavitation analysis are given on figures 19 through 22.

Pressures on the Stilling Basin Walls

Using the tailwater elevation curve furnished, the stilling basin formed an efficient hydraulic jump with adequate energy dissipation for discharges up to 2300 m³/s. Above this discharge, the stilling basin was adequate; however, weir flow occurred over the training walls of the stilling basin. The stilling basin operation for discharges of 1000, 2000, and 3600 m³/s is shown on figures 23, 24, and 25. The weir flow was due to the

* Arndt, R.E.A., J. W. Holl, J. C. Bohn, and W. T. Bechtel, "Influence of Surface Irregularities on Cavitation Performance," Journal of Ship Research, vol. 32, No. 3, pp. 157-170, September 1979.

high tailwater flowing over the walls into the stilling basin, where the higher velocity in the basin produced a lower water surface. To test instability of the stilling basin walls, pressures were measured along the inside and outside of the right wall. There was concern that the weir flow might produce a large pressure differential across the wall due to the subatmospheric pressures possible below the nappe of the flow.

To record pressures, 10 piezometers were installed along the right wall of the spillway stilling basin. The odd-numbered piezometers recorded pressures on the inside of the wall with the even-numbered ones on the outside. The locations by station and elevation are shown on figure 26. Pressures were initially taken using water manometers. These data indicated which piezometer locations produced the greater pressure fluctuations, which were then analyzed using 17.24-kPa pressure transducers and a recorder. Water manometer pressure data for the right wall of the spillway stilling basin are shown in the appendix (tables 1 to 6); transducer data are shown in tables 7 to 12. These data were believed similar for the left wall. All the piezometers on the outside of the wall recorded the tailwater height with only slight fluctuations due to wave action. The data recorded by the transducers were mostly above atmospheric pressure with only a few minimal subatmospheric pressures. Piezometer No. 9 registered some instantaneous subatmospheric pressures. The location of piezometer No. 9 at the toe of the hydraulic jump accounted for slight subatmospheric pressures on the order of 0.05 m with a maximum of 0.15 m. With the spillway, outlet works, and powerplant operating, piezometer No. 7 measured a minimal average subatmospheric pressure of 0.03 m at discharges of 2000, 2500, and 3000 m³/s. This was due to the weir flow over the wall at this point which produced subatmospheric pressures under the nappe. Piezometers No. 1, 3, and 5 recorded pressures above atmospheric. For the higher discharges above 3000 m³/s, the tailwater height overcame most of the weir flow effect. For the lower discharges of 1000 and 1500 m³/s, the tailwater was below the stilling basin walls.

No pressure fluctuations or subatmospheric pressures were formed large enough to produce a pressure differential which would endanger the stability of the basin walls. The effects of the weir flow should be minimal, provided the walls are designed for full hydrostatic pressure.

Riverbed Stabilization

The river channel was stabilized to study the velocities and erosion potential downstream of the hydraulic structures. The first step in the stabilization process was to form the riverbed with damp, compacted sand, using templates representing several river channel cross sections. This base was formed approximately 8.0 m below the actual channel outline. The channel was then brought to grade and stabilized with a surface layer of a 42:1 mixture (by weight) of sand to cement, respectively.

This mixture provided a good approximation of the reported weak sandstone of the riverbed downstream of the structures. The formed channel is shown on figure 27.

Velocity Profiles

With the stabilized riverbed, velocity measurements were made downstream of the spillway apron. The velocities were taken at or near the end of the apron (STA 1+550.0), and downstream at approximately 4 m (STA 1+554.0), and at 14 m (STA 1+564.0). The measurements above the riverbed varied with the tailwater height, with the exception of an initial measurement for each discharge at 0.5 m. Data were taken for each spillway test discharge. These data showed that all the velocities were within the design value of 5.0 m/s, with the exception of three instantaneous values (about 6.4 m/s) at 3600 m³/s. As shown in the graphical representations on figures 28 through 33, the velocities were, in general, lower along the centerline of the spillway and increasing on either side of the centerline.

Erosion Tests

These slightly higher velocities along the outer edges of the basin caused erosion at the left toe of the spillway apron for a discharge of 1000 m³/s. As the discharge increased, the erosion continued for 12.0 m downstream, producing minor undermining of the left

bank in this area. The undermining of the bank was accompanied by surface wave action which contributed to the bank erosion, extending the eroded area to approximately 24.4 m downstream of the apron. This erosion damage is shown on figure 34.

The eroded material was deposited in three places. For discharges up to 1500 m³/s, the eroded material was drawn up onto the apron by the stilling basin action, where it alternately collected immediately downstream of the end sill, and eventually washed out. Material eroded by the higher discharges remained on the apron as shown on figure 35. The material was also deposited behind the left spillway training wall from STA 1+434.45 to STA 1+448.67 when the tailwater elevation was above 34 m, as shown on figure 36. Another point of deposition for all discharges (fig. 37) was 134.0 m downstream of the spillway apron at about STA 1+684.0 where the material formed a bar across the river channel. The formation of a bar across the channel could cause a slightly higher tailwater in the powerplant tailrace. The tailwater elevation was 20.7 m for powerplant operation only. The height of the bar formed across the channel was between 2 and 3 m.

THE OUTLET WORKS MODEL

Diversion Condition

The diversion structure consisted of two 9-m-diameter concrete-lined tunnels. The open end of the 9-m conduit served as the intake for tunnel No. 1. The intake for tunnel No. 2 was a horseshoe-shaped bellmouth with a transition to a 9-m circular tunnel. After diversion, tunnel No. 1 will be converted into a permanent selective withdrawal outlet works structure. The entrance of tunnel No. 2 will be plugged and a bellmouth entrance for the powerplant will be provided at EL 50.98. The stilling basin used for tunnel No. 2 will not be used after diversion. It will be filled with excess excavated material after completion of the permanent outlet works.

The diversion structures were tested at reservoir EL 30, 40, and 53. At reservoir EL 30, the total discharge through both tunnels was 593.6 m³/s; neither entrance was totally submerged (fig. 38). At reservoir EL 40 and 53, (figs. 39 and 40) the discharges were 1472.7 and 2007.9 m³/s, respectively. Also, both intakes were totally submerged and both tunnels flowed full. With a discharge of 1472.7 m³/s, vortices formed over both entrances. The vortex was larger and more persistent over the entrance to tunnel No. 1 than tunnel No. 2. At reservoir EL 53 no vortices formed; however, an occasional dimple formed on the water surface over tunnel No. 1. Under all discharge conditions (figs. 41, 42, and 43), the energy dissipation of the stilling basins was adequate. A discharge curve for both tunnels of the diversion is shown on figure 44.

Modified Entrance—Tunnel No. 1

With the completion of the diversion requirements, the selective withdrawal tower will be constructed and used as the intake for tunnel No. 1, the permanent outlet works. In the 1:50.62 scale model, this structure was modified to only include the three sluices at EL 22 without bellmouth entrances as shown on figure 45. The two outer sluices were 1.83 by 3.66 m with the center sluice 1.02 by 3.66 m. The selective withdrawal tower was a standard design in operation at several other outlet works structures; therefore, it was not studied in this model.

Permanent Outlet Works—Tunnel No. 1

The flow conditions in the tunnel bend and the stilling basin operation were studied with the reservoir operating at EL 85. Operating the intake gates at one-half, three-fourths, and fully open produced discharges of 190, 310, and 422 m³/s, respectively, without the powerplant operating. Operation of the powerplant and outlet works produced a slightly higher tailwater elevation, resulting in slightly lower discharges for each gate opening. These discharges were 190, 297, and 399 m³/s, respectively.

At these discharges, the centrifugal force caused the flow to shift to the outside of the tunnel bend (fig. 46). The flow oscillated for about 197 m downstream of the bend as typically shown on figure 47, but became symmetrical prior to reaching the stilling basin. Pressures were measured along the tunnel bend with piezometers attached to a manometer board. The piezometers were located at the upstream end of the bend at STA 1+224.30, the point of maximum deflection, STA 1+263.20, and downstream of the bend at STA 1+352.18. No subatmospheric or excessively high pressures were noted. The pressure data are shown in table 13. The tunnel did not flow full during the tests.

Velocities and Erosion Downstream of the Stilling Basins and Powerplant

The outlet works stilling basin was adequate for all discharges. Figure 48 shows the stilling basin operating at a maximum discharge of 442 m³/s. Erosion tests were made on the outlet works model downstream of the stilling basins and the powerplant. The stabilized outlet works model riverbed is depicted on figure 49. Tests included the individual operation of the diversion structures, the outlet works, the powerplant, and combined outlet works and powerplant.

No erosion occurred when the diversion structures were tested at discharges of 593.6, 1472.7, and 2007.9 m³/s. No erosion was observed downstream of the outlet works, with or without the powerplant operating, when operated at reservoir elevation 85 and the spillway gates fully open. This observation was verified by the low velocities measured downstream of the stilling basin. Operation of the powerplant at a discharge of 250 m³/s and a tailwater of 21 or 22 m did not produce high velocities or erosion. The velocity measurements recorded downstream of the outlet works and powerplant shown on figures 50, 51, 52, and 53 were within the design range of 5 m/s.

Powerplant Intake

The model was tested at a discharge of 250 m³/s using the intake gates to control the reservoir elevation. These gates were used to control the flow since penstock studies had not

been requested as part of the model study and, consequently, downstream control had not been included in the model. The bellmouth intake structure is shown on figure 54.

The powerplant intake (tunnel No. 2) was tested for vortex formation at reservoir EL 60, 65, 70, 75, 80, and 85. The intake was tested initially without the trashrack structure. Very persistent vortices formed at reservoir EL 60 and 65 at a discharge of 250 m³/s. At both these water surface elevations, the vortices entrained air down through the gates. These vortices continued to the higher water surface ELS 70, 75, 80, and 85. However, the vortices became weaker and less persistent at the higher reservoir elevations. At reservoir EL 80 and 85 when the water surface was disturbed, the vortices dissipated and would not re-form. Figures 55, 56, 57, and 58 show the vortices formed over the powerplant entrance without the trashrack. At a discharge of 100 m³/s for reservoir EL 60 and 65 no vortices formed.

Trashrack Structure

The structural supports of the trashrack were constructed to scale with the prototype racks modeled using a fine mesh screen representing an opening of 0.10 by 0.10 m. The bellmouth entrance with the trashrack was tested at the same discharge and elevations. At reservoir EL 60 and 65 and a discharge of 250 m³/s, vortices formed at the upstream face of the trashrack and dissipated as they traveled toward the center of the structure. No vortices were observed at these elevations at a discharge of 100 m³/s. Vortices were suppressed at all reservoir elevations above the top of the trashrack structure. Flow at EL 60, 75, and 85 are shown on figures 59, 60, and 61.

Table 1.-*Water manometer pressure data for the right wall of the spillway stilling basin, spillway $Q = 1000 \text{ m}^3/\text{s}$, spillway-powerplant-outlet works $Q = 1650 \text{ m}^3/\text{s}$*

Piezometer No.*	Zero EL (m)	Spillway			Spillway-Powerplant-Outlet Works		
		$Q = 1000 \text{ m}^3/\text{s}$		TW = 21.1 m	$Q = 1650 \text{ m}^3/\text{s}$		TW = 31.4 m
		Manometer Readings (m)					
		Low	Mean	High	Low	Mean	High
1	34.36		33.63			33.63	
2	34.12		32.90			32.90	
3	26.32	26.56	26.93	27.29	27.29	27.66	28.02
4	26.07		26.81			27.54	
5	18.76	26.56	26.93	27.29	27.29	27.66	28.02
6	18.27		27.05			27.54	
7	34.36		33.88			34.12	
8	33.39		32.66			32.66	
9	25.59		25.59			25.59	
10	25.10		27.05			27.54	

* Even numbers located on inside face of wall, odd numbers of outside face.

Table 2.-*Water manometer pressure data for the right wall of the spillway stilling basin, spillway $Q = 1500 \text{ m}^3/\text{s}$, spillway-powerplant-outlet works $Q = 2150 \text{ m}^3/\text{s}$*

Piezometer No.*	Zero EL (m)	Spillway			Spillway-Powerplant-Outlet Works		
		$Q = 1500 \text{ m}^3/\text{s}$		TW = 30.4 m	$Q = 2150 \text{ m}^3/\text{s}$		TW = 34.3 m
		Manometer Readings (m)					
		Low	Mean	High	Low	Mean	High
1	34.36		33.88			34.12	
2	34.12		33.15			33.15	
3	26.32	29.49	29.97	30.46	29.73	30.22	30.70
4	26.07		30.22			30.70	
5	18.76	29.24	29.73	30.22	29.73	30.22	30.70
6	18.27		30.22			30.70	
7	34.36		33.88			33.88	
8	33.39		32.90			32.90	
9	25.59	26.32	26.93	27.54	26.80	27.42	28.02
10	25.10		30.22			30.70	

* Even numbers located on inside face of wall, odd numbers of outside face.

Table 3.-*Water manometer pressure data for the right wall of the spillway stilling basin, spillway $Q = 2000 \text{ m}^3/\text{s}$, spillway-powerplant-outlet works $Q = 2650 \text{ m}^3/\text{s}$*

Piezometer No.*	Zero EL (m)	Spillway			Spillway-Powerplant-Outlet Works		
		$Q = 2000 \text{ m}^3/\text{s}$		TW = 33.4 m	$Q = 2650 \text{ m}^3/\text{s}$		TW = 37.0 m
		Manometer Readings (m)					
		Low	Mean	High	Low	Mean	High
1	34.36	34.12	34.36	34.61	34.12	34.36	34.61
2	34.12		34.12		33.63	33.76	33.88
3	26.32	33.15	33.63	33.88	32.41	32.78	33.14
4	26.07		34.12			33.39	
5	18.76	32.66	33.27	33.88	32.41	32.78	33.14
6	18.27		34.12			33.39	
7	34.36		34.12			34.12	
8	33.39		34.12			33.63	
9	25.59	30.22	30.71	31.19	29.49	30.10	30.71
10	25.10		34.12			33.39	

* Even numbers located on inside face of wall, odd numbers of outside face.

Table 4.-*Water manometer pressure data for the right wall of the spillway stilling basin, spillway $Q = 2500 \text{ m}^3/\text{s}$, spillway-powerplant-outlet works $Q = 3150 \text{ m}^3/\text{s}$*

Piezometer No.*	Zero EL (m)	Spillway			Spillway-Powerplant-Outlet Works		
		$Q = 2500 \text{ m}^3/\text{s}$		TW = 36.2 m	$Q = 3150 \text{ m}^3/\text{s}$		TW = 39.5 m
		Manometer Readings (m)					
		Low	Mean	High	Low	Mean	High
1	34.36	36.56	36.80	37.05	36.80	37.17	37.53
2	34.12	36.32	36.56	36.80	36.32	36.56	36.80
3	26.32	35.34	36.95	36.56	35.10	36.95	36.80
4	26.07		36.80			36.93	
5	18.76	35.10	36.95	36.80	34.85	35.46	36.07
6	18.27		36.80			36.93	
7	34.36	33.63	33.88	34.12	33.88	34.00	34.12
8	33.39	36.56	36.68	36.80	36.56	36.80	37.05
9	25.59	33.15	33.88	34.61	32.66	33.51	34.36
10	25.10		36.80			36.93	

* Even numbers located on inside face of wall, odd numbers of outside face.

Table 5.-*Water manometer pressure data for the right wall of the spillway stilling basin, spillway $Q = 3000 \text{ m}^3/\text{s}$, spillway-powerplant-outlet works $Q = 3650 \text{ m}^3/\text{s}$*

Piezometer No.*	Zero EL (m)	Spillway			Spillway-Powerplant-Outlet Works		
		$Q = 3000 \text{ m}^3/\text{s}$		TW = 38.7 m	$Q = 3650 \text{ m}^3/\text{s}$		TW = 41.6 m
		Manometer Readings (m)					
		Low	Mean	High	Low	Mean	High
1	34.36	38.51	38.87	39.24	38.75	39.12	39.48
2	34.12	37.78	38.20	38.63	38.27	38.51	38.75
3	26.32	37.29	37.78	38.27	38.02	39.24	38.75
4	26.07		38.99			39.48	
5	18.76	37.29	37.78	38.27	38.02	38.44	38.87
6	18.27		38.99			39.48	
7	34.36	33.27	34.36	35.58	35.10	35.46	35.83
8	33.39	38.27	38.51	38.75	38.63	38.87	39.12
9	25.59	36.92	36.07	35.58	39.73	40.27	40.83
10	25.10		38.99			40.58	

* Even numbers located on inside face of wall, odd numbers of outside face.

Table 6.-*Water manometer pressure data for the right wall of the spillway stilling basin, spillway $Q = 3600 \text{ m}^3/\text{s}$, spillway-powerplant-outlet works $Q = 4250 \text{ m}^3/\text{s}$*

Piezometer No.*	Zero EL (m)	Spillway			Spillway-Powerplant-Outlet Works		
		$Q = 3600 \text{ m}^3/\text{s}$		TW = 41.0 m	$Q = 4250 \text{ m}^3/\text{s}$		TW = 44.3 m
		Manometer Readings (m)					
		Low	Mean	High	Low	Mean	High
1	34.36	39.97	40.22	40.46	40.22	40.46	40.70
2	34.12	39.73	39.97	40.22	40.22		40.95
3	26.32	39.48	39.97	40.46	39.73		40.46
4	26.07		40.95			41.31	
5	18.76	39.48	39.97	40.46	39.73	39.97	40.22
6	18.27		40.83			41.19	
7	34.36	36.80	37.41	38.02	37.78		38.51
8	33.39	39.73	40.09	40.46	40.22	40.46	40.70
9	25.59	39.73	40.09	40.46	40.70	40.95	41.19
10	25.10		40.95			41.31	

* Even numbers located on inside face of wall, odd numbers of outside face.

Table 7.-*Transducer pressure data for the right wall of the spillway stilling basin, spillway $Q = 1000 \text{ m}^3/\text{s}$, spillway-powerplant-outlet works $Q = 1650 \text{ m}^3/\text{s}$*

Piezometer No.*	Zero EL (m)	Spillway			Spillway-Powerplant-Outlet Works		
		$Q = 1000 \text{ m}^3/\text{s}$		TW = 27.1 m	$Q = 1650 \text{ m}^3/\text{s}$		TW = 31.4 m
		Manometer Readings (m)					
		Low	Mean	High	Low	Mean	High
1	34.36	34.36	34.36	34.36	34.36	34.36	34.36
3	26.32	26.42	26.40	26.40	26.42	26.40	26.39
5	18.76	18.98	18.97	18.96	18.88	18.88	18.86
7	34.36	34.36	34.36	34.36	34.36	34.36	34.36
8	33.39	33.39	33.39	33.39	33.39	33.39	33.39
9	25.59	25.61	25.60	25.59	25.68	25.60	25.67

* Even numbers located on inside face of wall, odd numbers of outside face.

Table 8.-*Transducer pressure data for the right wall of the spillway stilling basin, spillway $Q = 1500 \text{ m}^3/\text{s}$, spillway-powerplant-outlet works $Q = 2150 \text{ m}^3/\text{s}$*

Piezometer No.*	Zero EL (m)	Spillway			Spillway-Powerplant-Outlet Works		
		$Q = 1500 \text{ m}^3/\text{s}$		TW = 30.4 m	$Q = 2150 \text{ m}^3/\text{s}$		TW = 34.3 m
		Manometer Readings (m)					
		Low	Mean	High	Low	Mean	High
1	34.36	34.36	34.36	34.36	34.36	34.36	34.36
3	26.32	26.32	26.40	26.36	26.46	26.43	26.41
5	18.76	18.92	18.90	18.87	18.93	18.91	18.88
7	34.36	34.36	34.36	34.36	34.36	34.36	34.36
8	33.39	33.39	33.39	33.39	33.39	33.39	33.39
9	25.59	25.79	25.60	25.44	25.84	25.62	25.46

* Even numbers located on inside face of wall, odd numbers of outside face.

Table 9.-*Transducer pressure data for the right wall of the spillway stilling basin, spillway $Q = 2000 \text{ m}^3/\text{s}$, spillway-powerplant-outlet works $Q = 2650 \text{ m}^3/\text{s}$*

Piezometer No.*	Zero EL (m)	Spillway			Spillway-Powerplant-Outlet Works		
		$Q = 2000 \text{ m}^3/\text{s}$		TW = 33.4 m	$Q = 2650 \text{ m}^3/\text{s}$		TW = 37.0 m
		Manometer Readings (m)					
		Low	Mean	High	Low	Mean	High
1	34.36	34.48	34.44	34.43	34.41	34.39	34.37
3	26.32	26.45	26.43	26.38	26.45	26.43	26.39
5	18.76	18.94	18.90	18.84	18.93	18.90	18.87
7	34.36	34.52	34.47	34.45	34.36	34.33	34.32
8	33.39	33.39	33.39	33.39	33.39	33.39	33.39
9	25.59	25.76	25.62	25.51	25.80	25.62	25.50

* Even numbers located on inside face of wall, odd numbers of outside face.

Table 10.-*Transducer pressure data for the right wall of the spillway stilling basin, spillway $Q = 2500 \text{ m}^3/\text{s}$, spillway-powerplant-outlet works $Q = 2900 \text{ m}^3/\text{s}$*

Piezometer No.*	Zero EL (m)	Spillway			Spillway-Powerplant-Outlet Works		
		$Q = 2500 \text{ m}^3/\text{s}$		TW = 36.2 m	$Q = 2900 \text{ m}^3/\text{s}$		TW = 38.2 m
		Manometer Readings (m)					
		Low	Mean	High	Low	Mean	High
1	34.36	34.48	34.45	34.43	34.46	34.40	34.38
3	26.32	26.45	26.43	26.37	26.45	26.43	26.37
5	18.76	19.00	18.97	18.92	19.08	18.97	18.93
7	34.36	34.53	34.48	34.46	34.36	34.33	34.32
8	33.39	33.55	33.53	33.51	33.49	33.47	33.45
9	25.59	25.92	25.71	25.52	25.90	25.71	25.54

* Even numbers located on inside face of wall, odd numbers of outside face.

Table 11.—*Transducer pressure data for the right wall of the spillway stilling basin, spillway $Q = 3000 \text{ m}^3/\text{s}$, spillway-powerplant-outlet works $Q = 3400 \text{ m}^3/\text{s}$*

Piezometer No.*	Zero EL (m)	Spillway			Spillway-Powerplant-Outlet Works		
		$Q = 3000 \text{ m}^3/\text{s}$		TW = 38.7 m	$Q = 3400 \text{ m}^3/\text{s}$		TW = 40.6 m
		Manometer Readings (m)					
		Low	Mean	High	Low	Mean	High
1	36.34	36.46	36.42	36.37	36.44	36.40	36.36
3	26.32	26.52	26.50	26.45	26.48	26.46	26.42
5	18.76	19.03	19.01	18.99	19.03	19.01	19.00
7	36.34	36.53	36.48	36.39	36.37	36.32	36.29
8	33.39	33.79	33.77	33.75	33.61	33.57	33.55
9	25.59	25.97	25.77	25.63	26.01	25.83	25.69

* Even numbers located on inside face of wall, odd numbers of outside face.

Table 12.—*Transducer pressure data for the right wall of the spillway stilling basin, spillway $Q = 3600 \text{ m}^3/\text{s}$, spillway-powerplant-outlet works $Q = 4000 \text{ m}^3/\text{s}$*

Piezometer No.*	Zero EL (m)	Spillway			Spillway-Powerplant-Outlet Works		
		$Q = 3600 \text{ m}^3/\text{s}$		TW = 41.0 m	$Q = 4000 \text{ m}^3/\text{s}$		TW = 43.0 m
		Manometer Readings (m)					
		Low	Mean	High	Low	Mean	High
1	36.34	36.47	36.42	36.36	36.47	36.42	36.37
3	26.32	26.53	26.48	26.37	26.52	26.49	26.41
5	18.76	19.05	19.03	19.01	19.04	19.03	19.01
7	36.34	36.45	36.40	36.32	36.52	36.44	36.37
8	33.39	33.61	33.59	33.55	33.62	33.59	33.57
9	25.59	26.02	25.79	25.64	26.08	25.87	25.70

* Even numbers located on inside face of wall, odd numbers of outside face.

Table 13.-*Water manometer pressure data in the outlet works tunnel bend*

Piezometer No.	Zero EL (mm)	Manometer readings (mm)	Pressure head	
			Model (mm)	Prototype (m)
1	70.10	115.82	45.72	2.31
2	67.06	118.87	51.82	2.62
3	97.54	103.63	6.10	0.31
4	118.87	149.35	30.48	1.54
5	60.96	73.15	12.19	0.62
6	76.20	79.25	3.05	0.15
7	64.01	106.68	42.67	2.16
8	51.82	79.25	27.43	1.39
9	76.20	97.54	21.34	1.08

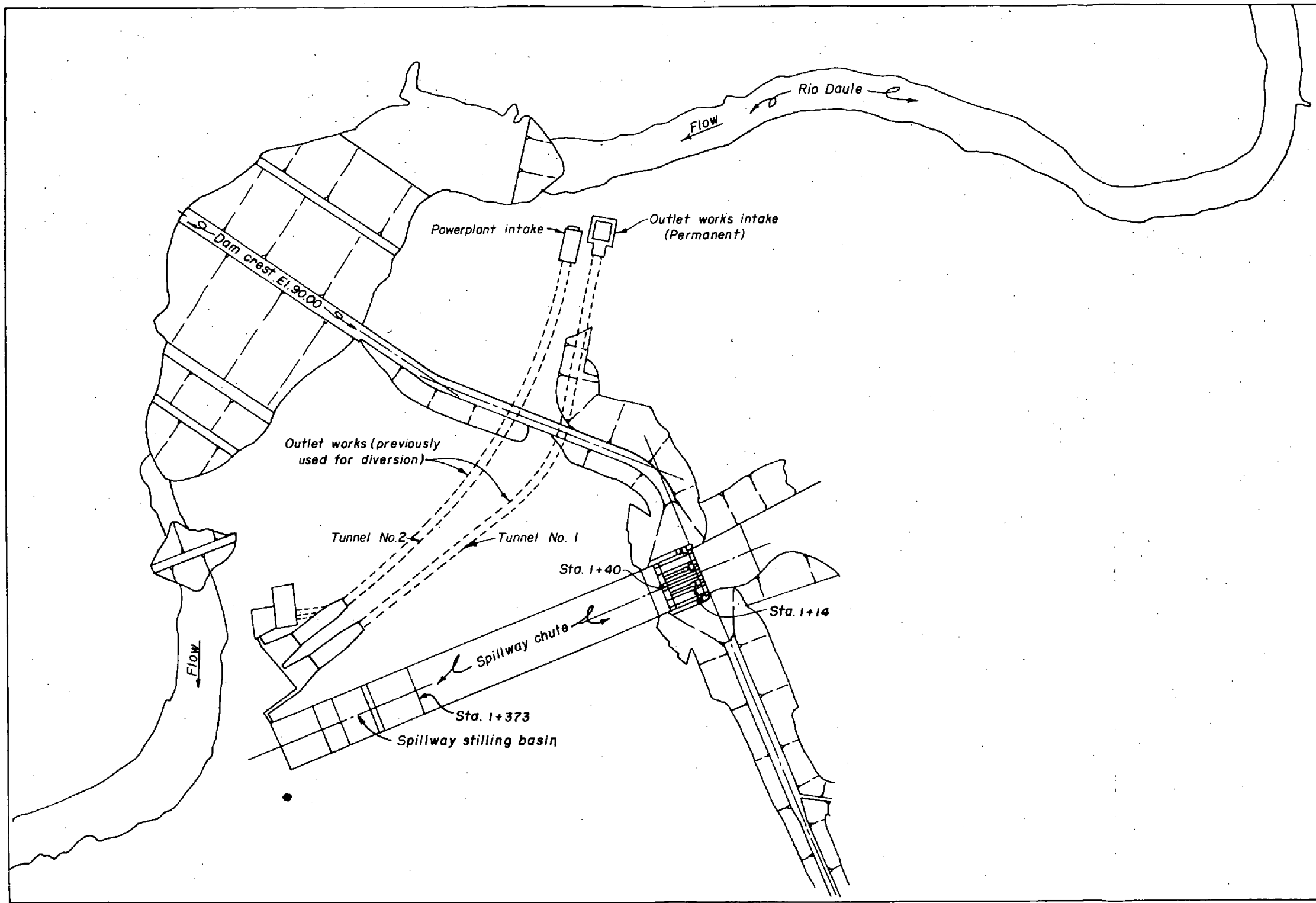


Figure 1.—General project plan.

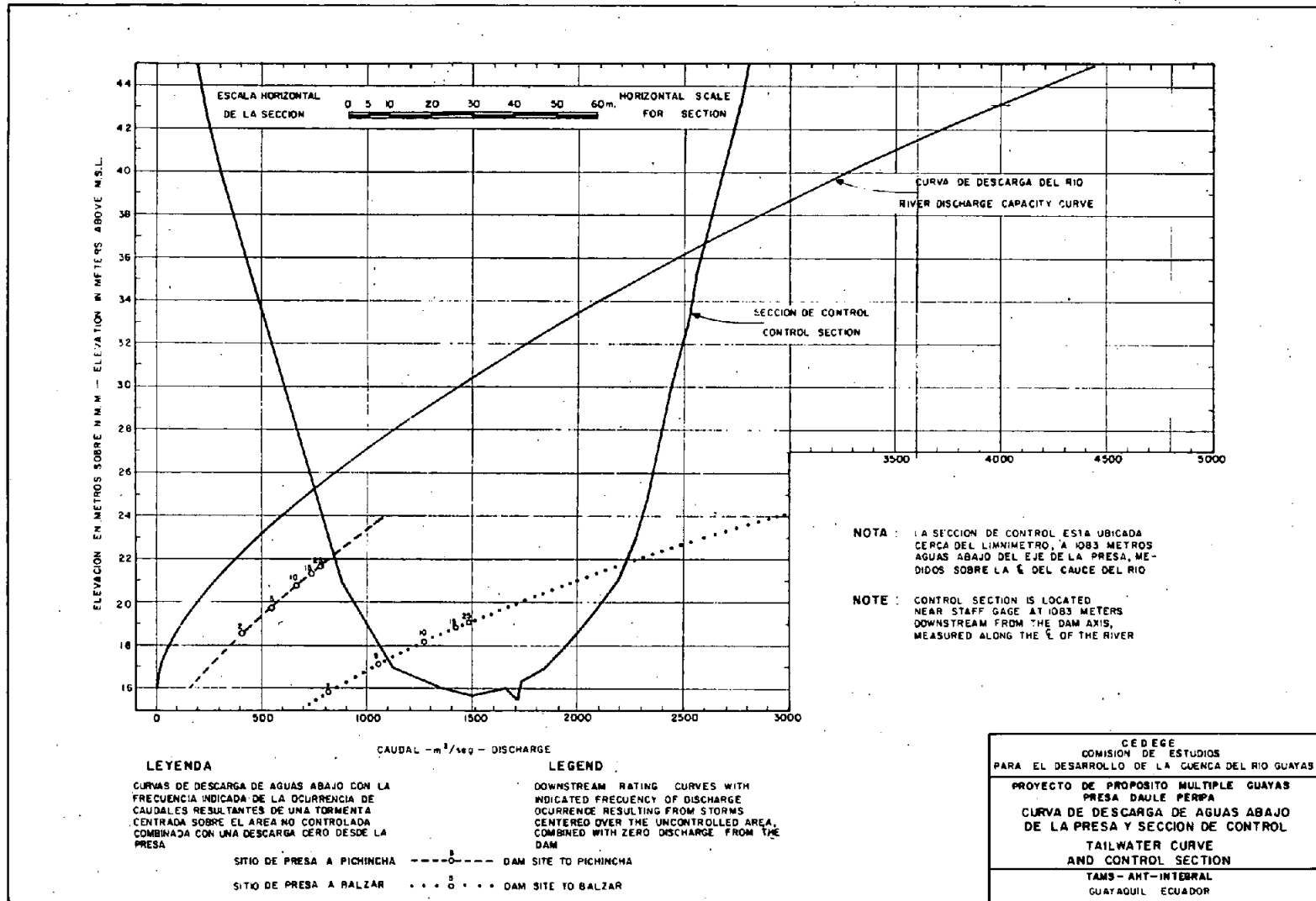


Figure 4.—Tailwater curve.

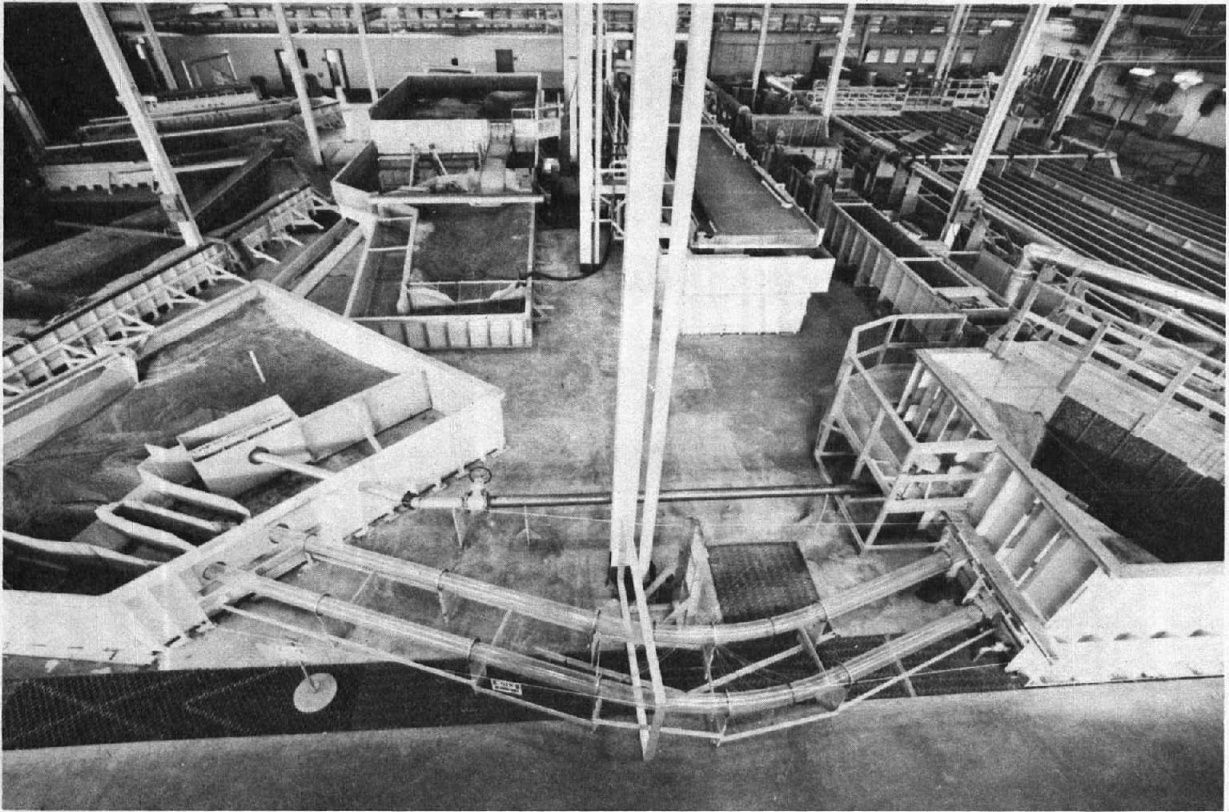


Figure 5.—Overall view of the 1:50.62 outlet works model in foreground; 1:80 spillway model in background.
P801-D-79578.

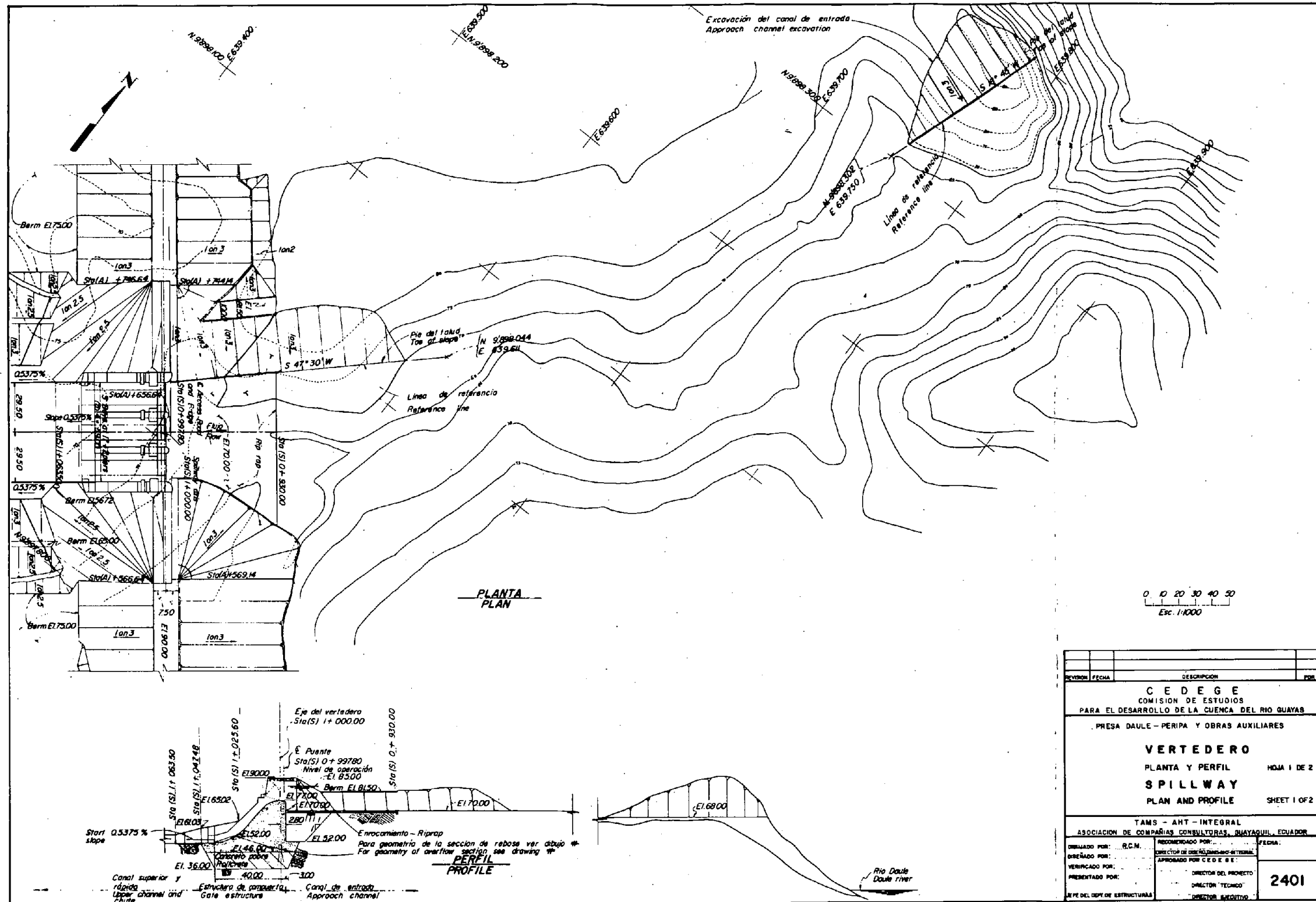


Figure 6.—Spillway plan and section showing proposed excavation of approach channel.



Figure 7.—Approach channel with proposed excavation filled in, located about 500 m upstream of spillway crest. P801-D-79579.

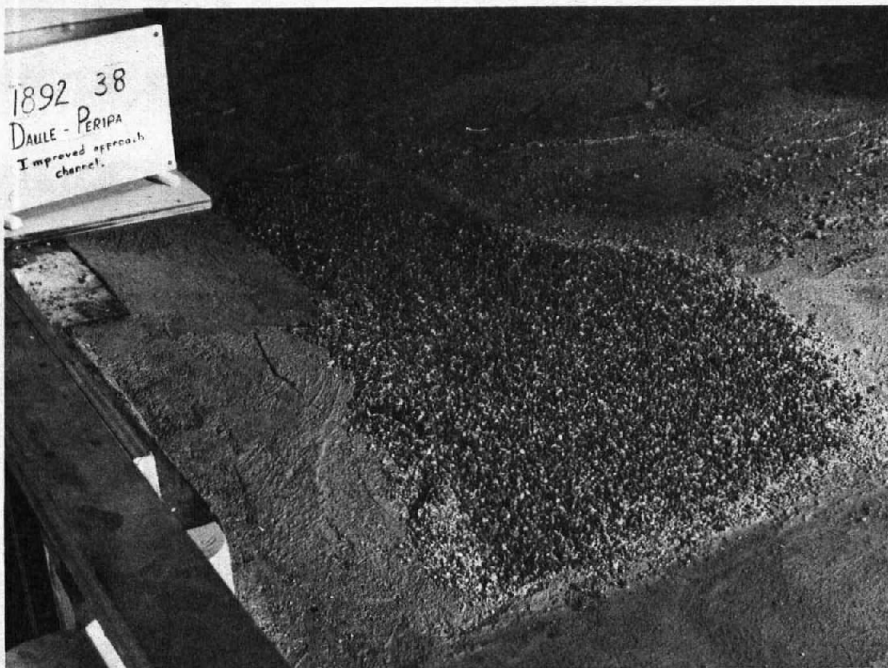


Figure 8.—Right side of approach channel adjacent to crest, with original topography restored. P801-D-79580.



Figure 9.—Flow pattern adjacent to crest: $Q = 2000 \text{ m}^3/\text{s}$ for the improved channel. P801-D-79581.

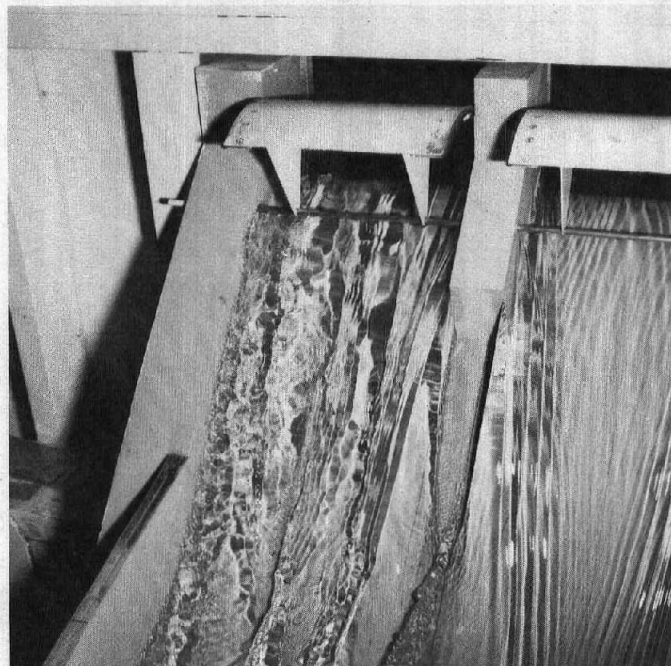


Figure 10.—Impingement of flow on the gate trunnions: $Q = 2600 \text{ m}^3/\text{s}$. P801-D-79582.

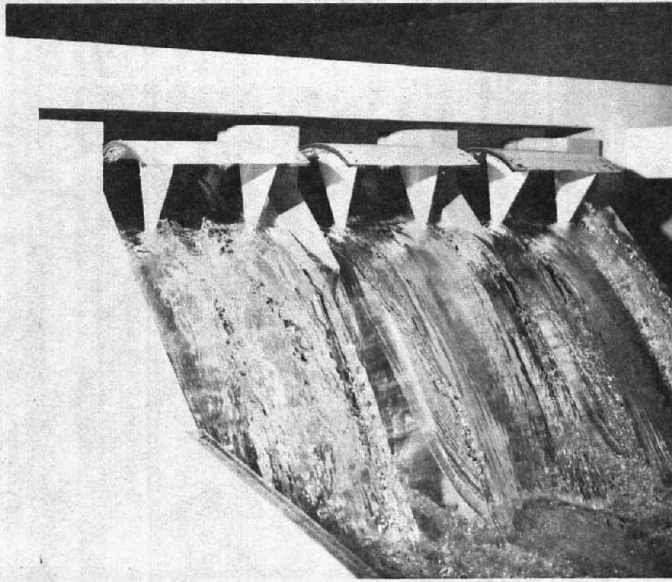


Figure 11.—Submergence of all trunnions: $Q = 3600 \text{ m}^3/\text{s}$.
P801-D-79583.



Figure 12.—Piers streamlined and shortened
to STA 1 + 20.5. P801-D-79584.

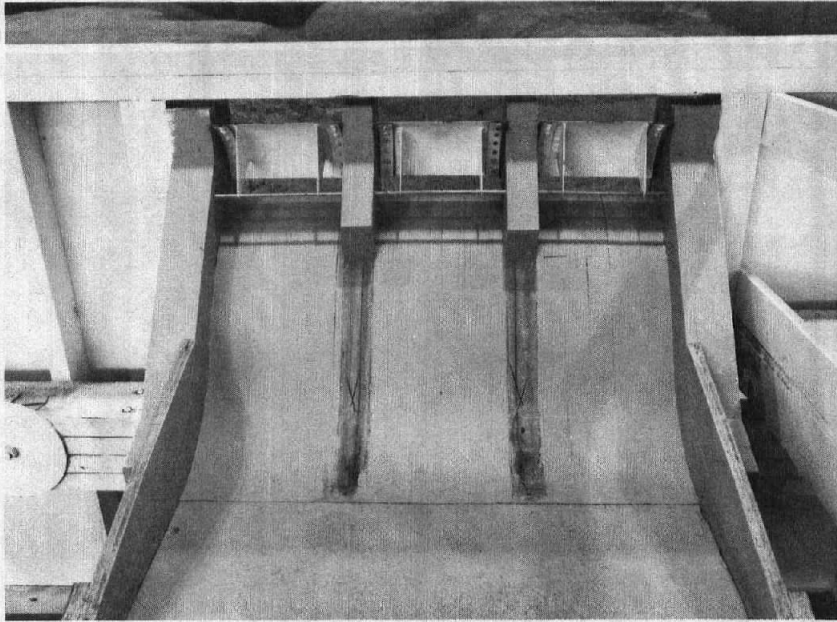


Figure 13.—Piers shortened to trunnion supports. P801-D-79585.

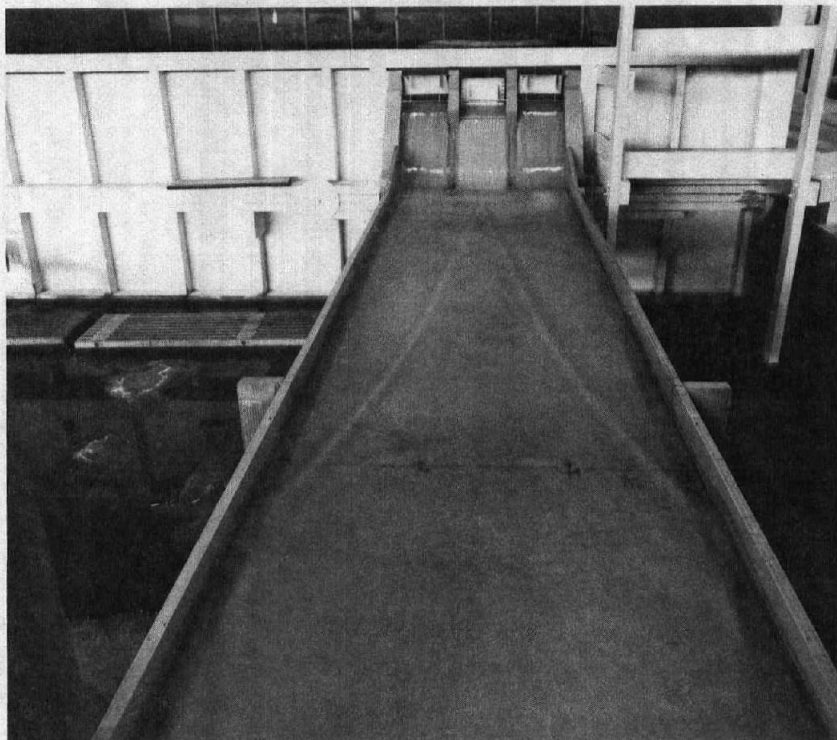


Figure 14.—Flow with recommended gate openings for $Q = 1000 \text{ m}^3/\text{s}$.
P801-D-79586.

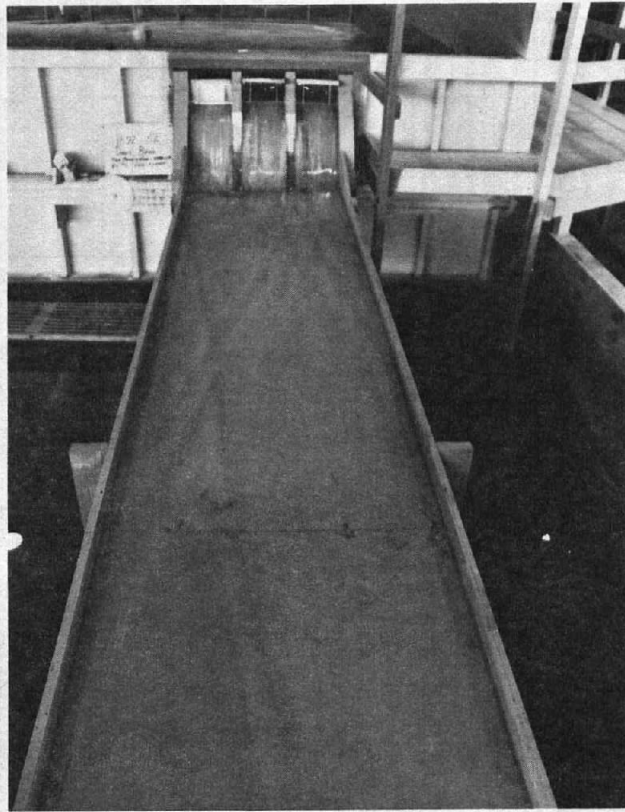


Figure 15.—Flow with recommended gate openings for $Q = 2000 \text{ m}^3/\text{s}$. P801-D-79587.

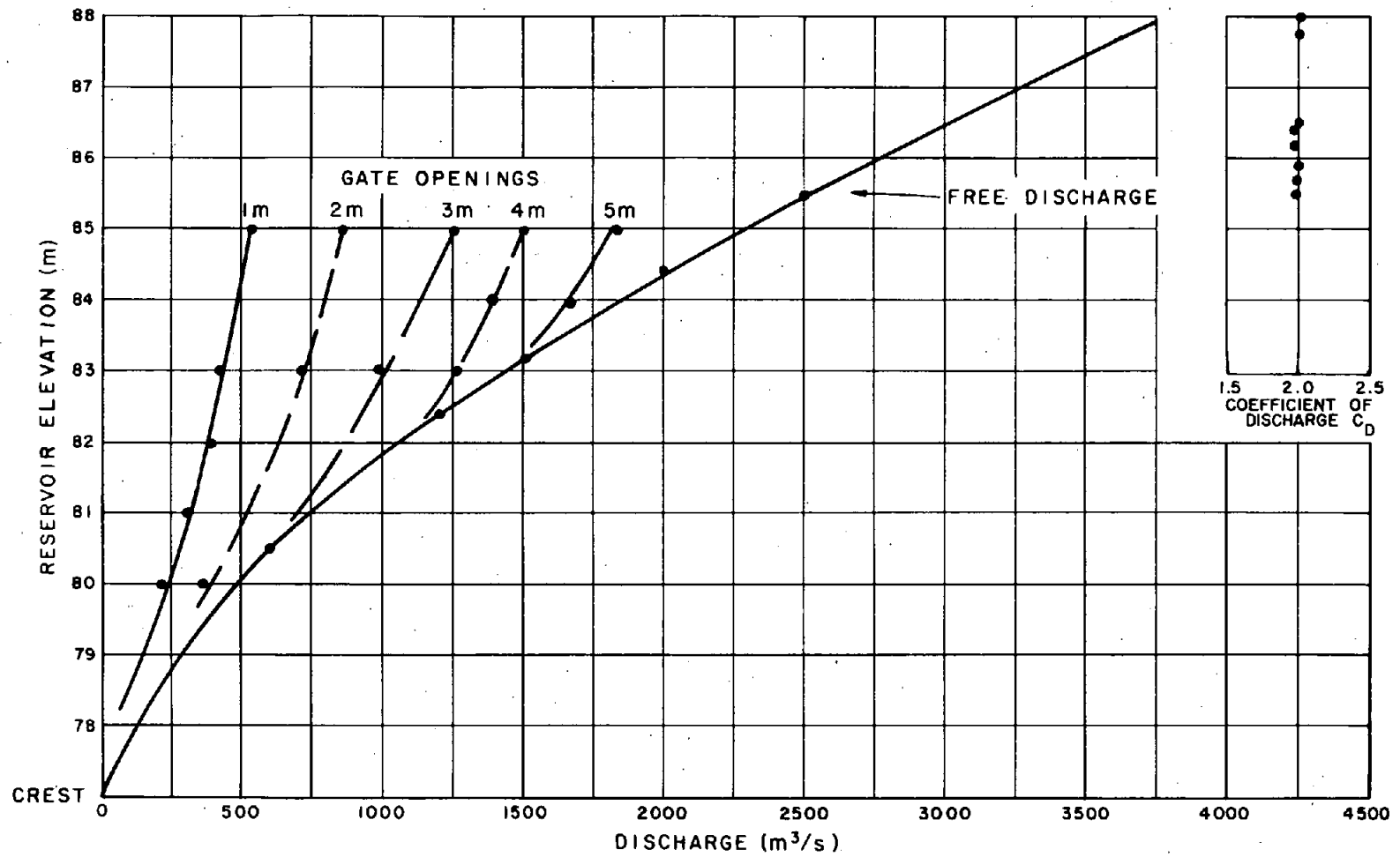


Figure 16.—Discharge curve for gate controlled and uncontrolled crest.

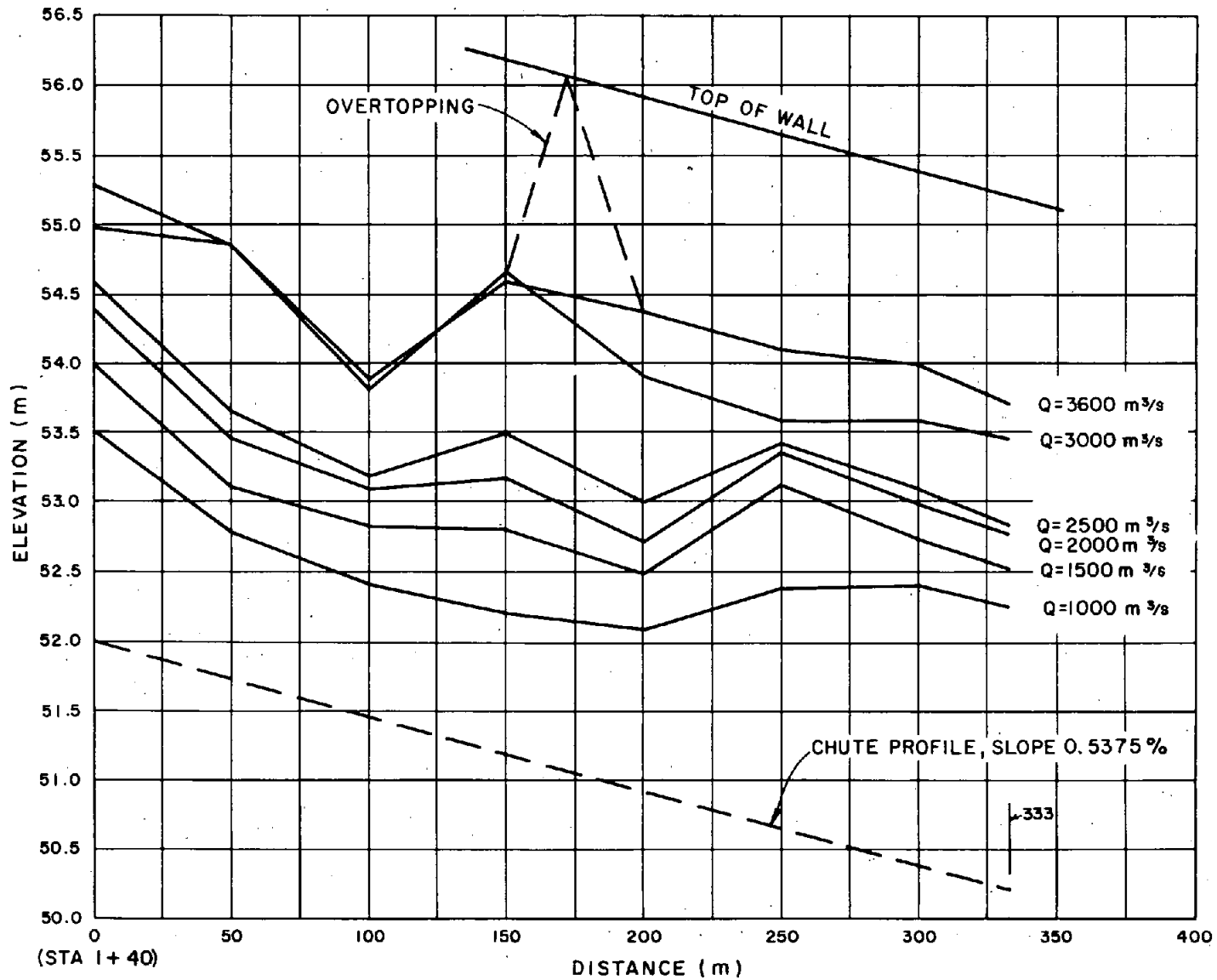


Figure 17.—Water surface profiles for the left wall of the spillway chute.

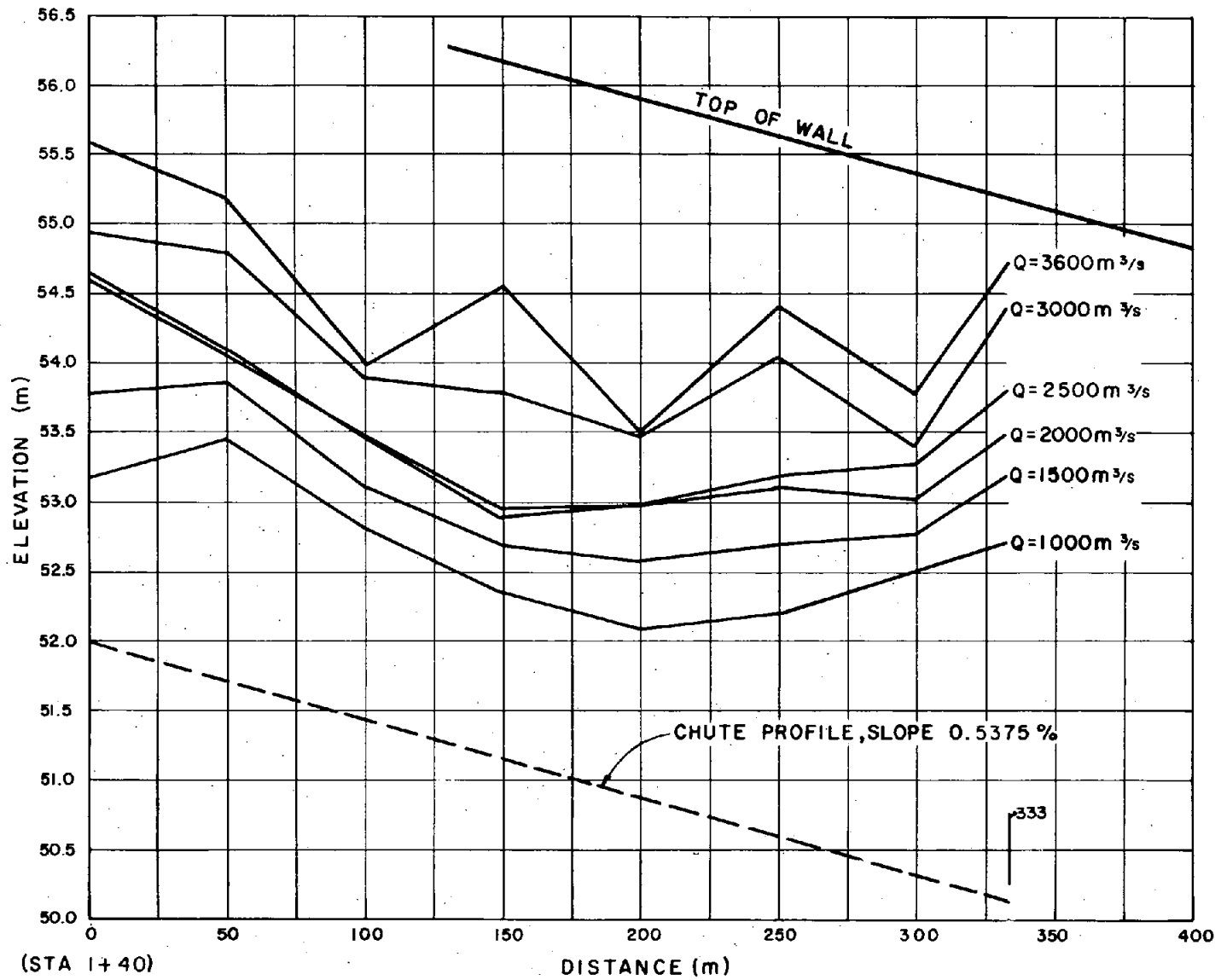


Figure 18.—Water surface profiles for the right wall of the spillway chute.

DAULE-PERIPA SPILLWAY

Q = 200.000 CMS INITIAL DEPTH = .140 M RUGSITY = 1.1000 MM N = .0128

STATION M	INVERT ELEV M	SLOPE	DEPTH M	VELOCITY M/SEC	PIEZ M	ENERGY GRADE LINE M	Q AIR/Q WATER	PROFILE	DEPTH NORMAL M	DEPTH CRITICAL M	THICKNESS BOUNDARY LAYER M
1040.00	52.000	.0054	.140	24.213	.140	85.020	0.000	S3	.771	1.088	.140
SURFACE SUFFICIENTLY ROUGH TO CAVITATE 1 TO 11 CHAMFERS REQUIRED											
1050.00	51.950	.0050	.169	20.103	.169	74.783	2.846	S3	.789	1.088	.169
CAVITATION WILL OCCUR FOR OFFSETS GREATER THAN .001 M 1 TO 7 CHAMFERS REQUIRED											
1060.00	51.890	.0060	.198	17.337	.196	68.942	1.344	S3	.745	1.088	.198
CAVITATION WILL OCCUR FOR OFFSETS GREATER THAN .004 M 1 TO 5 CHAMFERS REQUIRED											
1070.00	51.840	.0050	.221	15.318	.221	65.220	.850	S3	.789	1.088	.221
CAVITATION WILL OCCUR FOR OFFSETS GREATER THAN .009 M 1 TO 3 CHAMFERS REQUIRED											
1080.00	51.790	.0050	.246	13.771	.246	62.672	.586	S3	.789	1.088	.246
CAVITATION WILL OCCUR FOR OFFSETS GREATER THAN .018 M 1 TO 3 CHAMFERS REQUIRED											
1100.00	51.680	.0055	.295	11.494	.295	59.384	.306	S3	.765	1.088	.295
1125.00	51.540	.0056	.352	9.623	.352	57.085	.146	S3	.761	1.088	.352
1150.00	51.410	.0052	.406	8.356	.406	55.732	.063	S3	.779	1.088	.406
1175.00	51.270	.0056	.455	7.456	.455	54.842	0.000	S3	.761	1.088	.455
1200.00	51.140	.0052	.501	6.770	.501	54.211	0.000	S3	.779	1.088	.501
1225.00	51.010	.0052	.543	6.242	.543	53.738	0.000	S3	.779	1.088	.543
1250.00	50.870	.0056	.580	5.844	.580	53.365	0.000	S3	.761	1.088	.580
1275.00	50.740	.0052	.615	5.515	.615	53.060	0.000	S3	.779	1.088	.615
1300.00	50.600	.0056	.643	5.273	.643	52.802	0.000	S3	.761	1.088	.643
1325.00	50.470	.0052	.670	5.062	.670	52.577	0.000	S3	.779	1.088	.670
1350.00	50.330	.0056	.689	4.918	.689	52.376	0.000	S3	.761	1.088	.689
1373.00	50.210	.0052	.698	4.854	.671	52.203	0.000	S3	.778	1.082	.698
1390.00	47.980	.1312	.431	7.872	.386	51.842	0.000	S2	.286	1.086	.431

Figure 19.—Computer printout for cavitation analysis at Q = 200 m³/s.

 DAULE-PERIPA SPILLWAY

STATION M	INVERT ELEV M	SLOPE	DEPTH M	VELOCITY M/SEC	PIEZ M	ENERGY		PROFILE	DEPTH		THICKNESS BOUNDARY LAYER M
						GRADE LINE M	Q AIR/Q WATER		NORMAL M	CRITICAL M	
1400.00	44.660	.3320	.321	10.573	.258	51.188	0.000	S2	.218	1.102	.321
1410.00	39.870	.4790	.259	13.109	.183	49.690	0.000	S2	.197	1.122	.259
CAVITATION WILL OCCUR FOR OFFSETS GREATER THAN							.025 M	1 TO 2 CHAMFERS REQUIRED			
1420.00	33.590	.6280	.221	15.308	.139	46.870	0.000	S2	.185	1.148	.221
CAVITATION WILL OCCUR FOR OFFSETS GREATER THAN							.009 M	1 TO 3 CHAMFERS REQUIRED			
1426.04	29.080	.7487	.208	16.429	.119	44.338	0.000	S2	.179	1.168	.208
CAVITATION WILL OCCUR FOR OFFSETS GREATER THAN							.006 M	1 TO 4 CHAMFERS REQUIRED			

Figure 19.—Computer printout for cavitation analysis at $Q = 200 \text{ m}^3/\text{s}$ —Continued.

DAULE-PERIPA SPILLWAY

Q = 500.000 CMS INITIAL DEPTH = .351 M RUGOSITY = 1.000 MM N = .0132

STATION M	INVERT ELEV M	SLOPE	DEPTH M	VELOCITY M/SEC	PIEZ M	ENERGY GRADE LINE M	Q AIR/Q WATER	PROFILE	DEPTH NORMAL M	DEPTH CRITICAL M	THICKNESS BOUNDARY LAYER M
1040.00	52.000	.0054	.351	24.144	.351	85.044	0.000	S3	1.372	2.005	.256
SURFACE SUFFICIENTLY ROUGH TO CAVITATE 1 TO 11 CHAMFERS REQUIRED											
1050.00	51.950	.0050	.373	22.705	.373	81.234	.915	S3	1.405	2.005	.318
SURFACE SUFFICIENTLY ROUGH TO CAVITATE 1 TO 9 CHAMFERS REQUIRED											
1060.00	51.890	.0060	.395	21.450	.395	78.089	.878	S3	1.326	2.005	.378
CAVITATION WILL OCCUR FOR OFFSETS GREATER THAN .002 M 1 TO 8 CHAMFERS REQUIRED											
1070.00	51.840	.0050	.417	20.339	.417	75.458	.578	S3	1.405	2.005	.417
CAVITATION WILL OCCUR FOR OFFSETS GREATER THAN .002 M 1 TO 7 CHAMFERS REQUIRED											
1080.00	51.790	.0050	.438	19.350	.438	73.228	.471	S3	1.405	2.005	.438
CAVITATION WILL OCCUR FOR OFFSETS GREATER THAN .003 M 1 TO 6 CHAMFERS REQUIRED											
1100.00	51.880	.0055	.480	17.658	.480	69.647	.303	S3	1.363	2.004	.480
CAVITATION WILL OCCUR FOR OFFSETS GREATER THAN .006 M 1 TO 5 CHAMFERS REQUIRED											
1125.00	51.540	.0055	.531	15.960	.531	66.358	.176	S3	1.355	2.005	.531
CAVITATION WILL OCCUR FOR OFFSETS GREATER THAN .011 M 1 TO 4 CHAMFERS REQUIRED											
1150.00	51.410	.0052	.581	14.596	.581	63.938	.102	S3	1.387	2.005	.581
CAVITATION WILL OCCUR FOR OFFSETS GREATER THAN .021 M 1 TO 3 CHAMFERS REQUIRED											
1175.00	51.270	.0058	.628	13.485	.628	62.097	.029	S3	1.356	2.005	.628
CAVITATION WILL OCCUR FOR OFFSETS GREATER THAN .035 M 1 TO 2 CHAMFERS REQUIRED											
1200.00	51.140	.0052	.675	12.553	.675	60.652	0.000	S3	1.388	2.005	.675
CAVITATION WILL OCCUR FOR OFFSETS GREATER THAN .057 M 1 TO 2 CHAMFERS REQUIRED											
1225.00	51.010	.0052	.720	11.764	.720	59.492	0.000	S3	1.388	2.004	.720
1250.00	50.870	.0056	.764	11.097	.764	58.540	0.000	S3	1.355	2.005	.764
1275.00	50.740	.0052	.808	10.514	.808	57.745	0.000	S3	1.387	2.005	.808

Figure 20.—Computer printout for cavitation analysis at Q = 500 m³/s.

 DAULE-PERIPA SPILLWAY

STATION M	INVERT ELEV M	SLOPE	DEPTH M	VELOCITY M/SEC	PIEZ M	ENERGY GRADE LINE M	Q AIR/Q WATER	PROFILE	DEPTH		THICKNESS BOUNDARY LAYER M
									NORMAL M	CRITICAL M	
1300.00	50.600	.0056	.846	10.014	.846	57.071	0.000	S3	1.355	2.005	.846
1325.00	50.470	.0052	.886	9.568	.886	56.490	0.000	S3	1.387	2.005	.886
1350.00	50.330	.0056	.923	9.186	.923	55.985	0.000	S3	1.355	2.005	.923
1373.00	50.210	.0052	.942	8.995	.815	55.563	0.000	S3	1.388	1.984	.942
1390.00	47.980	.1312	.786	10.783	.640	55.142	0.000	S2	.505	1.992	.786
1400.00	44.680	.3320	.650	13.044	.468	54.671	0.000	S2	.384	2.023	.650
							CAVITATION WILL OCCUR FOR OFFSETS GREATER THAN	.042 M	1 TO 2 CHAMFERS REQUIRED		
1410.00	39.870	.4790	.545	15.558	.341	53.785	0.000	S2	.348	2.060	.545
							CAVITATION WILL OCCUR FOR OFFSETS GREATER THAN	.013 M	1 TO 3 CHAMFERS REQUIRED		
1420.00	33.590	.6280	.468	18.097	.252	52.208	0.000	S2	.326	2.106	.468
							CAVITATION WILL OCCUR FOR OFFSETS GREATER THAN	.005 M	1 TO 5 CHAMFERS REQUIRED		
1426.04	29.080	.7467	.433	19.577	.208	50.782	0.000	S2	.314	2.146	.433
							CAVITATION WILL OCCUR FOR OFFSETS GREATER THAN	.003 M	1 TO 6 CHAMFERS REQUIRED		

48

Figure 20.—Computer printout for cavitation analysis at Q = 500 m³/s—Continued.

DAULE-PERIPA SPILLWAY

Q = 1000.000 CMS INITIAL DEPTH = .706 M RUGOSITY = 1.1000 MM N = .0137

STATION M	INVERT ELEV M	SLOPE	DEPTH M	VELOCITY M/SEC	PIEZ M	ENERGY GRADE LINE M	Q AIR/Q WATER	PROFILE	DEPTH		THICKNESS BOUNDARY LAYER M
									NORMAL M	CRITICAL M	
1040.00	52.000	.0054	.706	24.007	.706	85.029	0.000	S3	2.134	3.182	.256
SURFACE SUFFICIENTLY ROUGH TO CAVITATE								1 TO 10 CHAMFERS REQUIRED			
1050.00	51.950	.0050	.725	23.379	.725	83.327	.221	S3	2.185	3.182	.317
SURFACE SUFFICIENTLY ROUGH TO CAVITATE								1 TO 9 CHAMFERS REQUIRED			
1060.00	51.890	.0060	.744	22.790	.744	81.761	.148	S3	2.061	3.182	.377
CAVITATION WILL OCCUR FOR OFFSETS GREATER THAN .001 M								1 TO 9 CHAMFERS REQUIRED			
1070.00	51.840	.0050	.762	22.230	.762	80.317	.153	S3	2.185	3.182	.435
CAVITATION WILL OCCUR FOR OFFSETS GREATER THAN .001 M								1 TO 8 CHAMFERS REQUIRED			
1080.00	51.790	.0050	.781	21.700	.781	78.980	.125	S3	2.185	3.182	.492
CAVITATION WILL OCCUR FOR OFFSETS GREATER THAN .002 M								1 TO 8 CHAMFERS REQUIRED			
1100.00	51.680	.0055	.818	20.725	.818	76.586	.057	S3	2.119	3.182	.602
CAVITATION WILL OCCUR FOR OFFSETS GREATER THAN .003 M								1 TO 7 CHAMFERS REQUIRED			
1125.00	51.640	.0056	.863	19.638	.863	74.031	.003	S3	2.107	3.182	.734
CAVITATION WILL OCCUR FOR OFFSETS GREATER THAN .004 M								1 TO 8 CHAMFERS REQUIRED			
1150.00	51.410	.0052	.908	18.671	.908	71.868	0.000	S3	2.159	3.182	.863
CAVITATION WILL OCCUR FOR OFFSETS GREATER THAN .006 M								1 TO 5 CHAMFERS REQUIRED			
1175.00	51.270	.0056	.952	17.813	.951	70.016	0.000	S3	2.108	3.182	.952
CAVITATION WILL OCCUR FOR OFFSETS GREATER THAN .008 M								1 TO 4 CHAMFERS REQUIRED			
1200.00	51.140	.0052	.995	17.038	.995	68.416	0.000	S3	2.159	3.182	.995
CAVITATION WILL OCCUR FOR OFFSETS GREATER THAN .011 M								1 TO 4 CHAMFERS REQUIRED			
1225.00	51.010	.0052	1.037	16.340	1.037	67.021	0.000	S3	2.158	3.182	1.037
CAVITATION WILL OCCUR FOR OFFSETS GREATER THAN .015 M								1 TO 4 CHAMFERS REQUIRED			
1250.00	50.870	.0056	1.079	15.712	1.079	65.794	0.000	S3	2.107	3.181	1.079
CAVITATION WILL OCCUR FOR OFFSETS GREATER THAN .020 M								1 TO 3 CHAMFERS REQUIRED			

Figure 21.—Computer printout for cavitation analysis at Q = 1000 m³/s.

 DAULE-PERIPA SPILLWAY

STATION M	INVERT ELEV M	SLOPE	DEPTH M	VELOCITY M/SEC	PIEZ M	ENERGY		PROFILE	DEPTH		THICKNESS BOUNDARY LAYER M
						GRADE LINE M	Q AIR/Q WATER		NORMAL M	CRITICAL M	
1275.00	50.740	.0052	1.120	15.136	1.120	64.708	0.000	S3	2.158	3.182	1.120
CAVITATION WILL OCCUR FOR OFFSETS GREATER THAN .026 M 1 TO 3 CHAMFERS REQUIRED											
1300.00	50.600	.0056	1.160	14.616	1.160	63.740	0.000	S3	2.107	3.182	1.160
CAVITATION WILL OCCUR FOR OFFSETS GREATER THAN .032 M 1 TO 3 CHAMFERS REQUIRED											
1325.00	50.470	.0052	1.199	14.133	1.199	62.871	0.000	S3	2.158	3.182	1.199
CAVITATION WILL OCCUR FOR OFFSETS GREATER THAN .041 M 1 TO 2 CHAMFERS REQUIRED											
1350.00	50.330	.0056	1.238	13.696	1.238	62.087	0.000	S3	2.107	3.182	1.238
CAVITATION WILL OCCUR FOR OFFSETS GREATER THAN .051 M 1 TO 2 CHAMFERS REQUIRED											
1373.00	50.210	.0052	1.249	13.975	.866	61.412	0.000	S3	2.156	3.132	1.249
CAVITATION WILL OCCUR FOR OFFSETS GREATER THAN .049 M 1 TO 2 CHAMFERS REQUIRED											
1390.00	47.980	.1312	1.154	14.688	.766	60.845	0.000	S2	.778	3.145	1.154
CAVITATION WILL OCCUR FOR OFFSETS GREATER THAN .028 M 1 TO 3 CHAMFERS REQUIRED											
1400.00	44.660	.3320	1.033	16.411	.607	60.371	0.000	S2	.590	3.198	1.033
CAVITATION WILL OCCUR FOR OFFSETS GREATER THAN .013 M 1 TO 4 CHAMFERS REQUIRED											
1410.00	39.870	.4790	.913	18.555	.466	59.645	0.000	S2	.535	3.258	.913
CAVITATION WILL OCCUR FOR OFFSETS GREATER THAN .006 M 1 TO 5 CHAMFERS REQUIRED											
1420.00	33.590	.6280	.810	20.930	.351	58.508	0.000	S2	.501	3.332	.810
CAVITATION WILL OCCUR FOR OFFSETS GREATER THAN .003 M 1 TO 7 CHAMFERS REQUIRED											
1428.04	29.080	.7467	.756	22.413	.289	57.540	0.000	S2	.483	3.397	.756
CAVITATION WILL OCCUR FOR OFFSETS GREATER THAN .002 M 1 TO 9 CHAMFERS REQUIRED											

50

Figure 21.—Computer printout for cavitation analysis at $Q = 1000 \text{ m}^3/\text{s}$ —Continued.

 DAULE-PERIPA SPILLWAY

Q = 2000.000 CMS INITIAL DEPTH = 1.428 M RUGOSITY = 1.0000 MM N = .0143

STATION M	INVERT ELEV M	SLOPE	DEPTH M	VELOCITY M/SEC	PIEZ M	ENERGY		PROFILE	DEPTH		THICKNESS BOUNDARY LAYER M
						GRADE LINE M	Q AIR/Q WATER		NORMAL M	CRITICAL M	
1040.00	52.000	.0054	1.428	23.738	1.428	85.031	0.000	S3	3.340	5.051	.257
SURFACE SUFFICIENTLY ROUGH TO CAVITATE								1 TO 9 CHAMFERS REQUIRED			
1050.00	51.950	.0050	1.444	23.470	1.444	84.288	0.000	S3	3.421	5.051	.318
SURFACE SUFFICIENTLY ROUGH TO CAVITATE								1 TO 9 CHAMFERS REQUIRED			
1060.00	51.890	.0060	1.460	23.212	1.460	83.568	0.000	S3	3.224	5.051	.377
CAVITATION WILL OCCUR FOR OFFSETS GREATER THAN .001 M								1 TO 8 CHAMFERS REQUIRED			
1070.00	51.840	.0050	1.477	22.957	1.477	82.873	0.000	S3	3.421	5.051	.435
CAVITATION WILL OCCUR FOR OFFSETS GREATER THAN .001 M								1 TO 8 CHAMFERS REQUIRED			
1080.00	51.790	.0050	1.493	22.708	1.493	82.203	0.000	S3	3.421	5.051	.491
CAVITATION WILL OCCUR FOR OFFSETS GREATER THAN .002 M								1 TO 8 CHAMFERS REQUIRED			
1100.00	51.680	.0055	1.525	22.233	1.525	80.927	0.000	S3	3.316	5.051	.600
CAVITATION WILL OCCUR FOR OFFSETS GREATER THAN .002 M								1 TO 7 CHAMFERS REQUIRED			
1125.00	51.540	.0056	1.564	21.672	1.564	79.445	0.000	S3	3.297	5.051	.730
CAVITATION WILL OCCUR FOR OFFSETS GREATER THAN .003 M								1 TO 7 CHAMFERS REQUIRED			
1150.00	51.410	.0052	1.604	21.140	1.604	78.076	0.000	S3	3.377	5.051	.856
CAVITATION WILL OCCUR FOR OFFSETS GREATER THAN .003 M								1 TO 8 CHAMFERS REQUIRED			
1175.00	51.270	.0056	1.642	20.642	1.642	76.808	0.000	S3	3.297	5.050	.978
CAVITATION WILL OCCUR FOR OFFSETS GREATER THAN .004 M								1 TO 8 CHAMFERS REQUIRED			
1200.00	51.140	.0052	1.681	20.167	1.681	75.630	0.000	S3	3.377	5.050	1.098
CAVITATION WILL OCCUR FOR OFFSETS GREATER THAN .005 M								1 TO 6 CHAMFERS REQUIRED			
1225.00	51.010	.0052	1.719	19.718	1.719	74.534	0.000	S3	3.377	5.051	1.216
CAVITATION WILL OCCUR FOR OFFSETS GREATER THAN .006 M								1 TO 5 CHAMFERS REQUIRED			
1250.00	50.870	.0056	1.757	19.298	1.757	73.512	0.000	S3	3.296	5.051	1.332
CAVITATION WILL OCCUR FOR OFFSETS GREATER THAN .007 M								1 TO 5 CHAMFERS REQUIRED			

Figure 22.—Computer printout for cavitation analysis at Q = 2000 m³/s.

 DAULE-PERIPA SPILLWAY

STATION M	INVERT ELEV M	SLOPE	DEPTH M	VELOCITY M/SEC	PIEZ M	ENERGY GRADE LINE M	Q AIR/Q WATER	PROFILE	DEPTH		THICKNESS BOUNDARY LAYER M
									NORMAL M	CRITICAL M	
1275.00	50.740	.0052	1.794	18.894	1.794	72.555	0.000	S3	3.377	5.051	1.448
CAVITATION WILL OCCUR FOR OFFSETS GREATER THAN							.009 M	1 TO 5 CHAMFERS REQUIRED			
1300.00	50.600	.0058	1.831	18.516	1.831	71.659	0.000	S3	3.296	5.051	1.559
CAVITATION WILL OCCUR FOR OFFSETS GREATER THAN							.010 M	1 TO 4 CHAMFERS REQUIRED			
1325.00	50.470	.0052	1.867	18.152	1.867	70.817	0.000	S3	3.377	5.051	1.670
CAVITATION WILL OCCUR FOR OFFSETS GREATER THAN							.012 M	1 TO 4 CHAMFERS REQUIRED			
1350.00	50.330	.0056	1.903	17.811	1.903	70.025	0.000	S3	3.296	5.051	1.780
CAVITATION WILL OCCUR FOR OFFSETS GREATER THAN							.014 M	1 TO 4 CHAMFERS REQUIRED			
1373.00	50.210	.0052	1.880	18.029	.864	69.304	0.000	S3	3.373	4.925	1.880
CAVITATION WILL OCCUR FOR OFFSETS GREATER THAN							.010 M	1 TO 5 CHAMFERS REQUIRED			
1390.00	47.980	.1312	1.799	18.848	.812	68.715	0.000	S2	1.204	4.950	1.799
CAVITATION WILL OCCUR FOR OFFSETS GREATER THAN							.008 M	1 TO 9 CHAMFERS REQUIRED			
1400.00	44.660	.3320	1.676	20.230	.669	68.281	0.000	S2	.911	5.034	1.878
CAVITATION WILL OCCUR FOR OFFSETS GREATER THAN							.005 M	1 TO 6 CHAMFERS REQUIRED			
1410.00	39.870	.4790	1.537	22.058	.535	67.693	0.000	S2	.825	5.135	1.537
CAVITATION WILL OCCUR FOR OFFSETS GREATER THAN							.003 M	1 TO 8 CHAMFERS REQUIRED			
1420.00	33.590	.6280	1.400	24.208	.411	66.862	0.000	S2	.773	5.259	1.400
CAVITATION WILL OCCUR FOR OFFSETS GREATER THAN							.001 M	1 TO 11 CHAMFERS REQUIRED			
1426.04	29.080	.7467	1.324	25.609	.338	66.195	0.000	S2	.745	5.365	1.324
SURFACE SUFFICIENTLY ROUGH TO CAVITATE								1 TO 13 CHAMFERS REQUIRED			

52

Figure 22.—Computer printout for cavitation analysis at Q = 2000 m³/s—Continued.



Figure 23.—Spillway stilling basin operation for $Q = 1000 \text{ m}^3/\text{s}$ and tailwater EL 25. P801-D-79588.

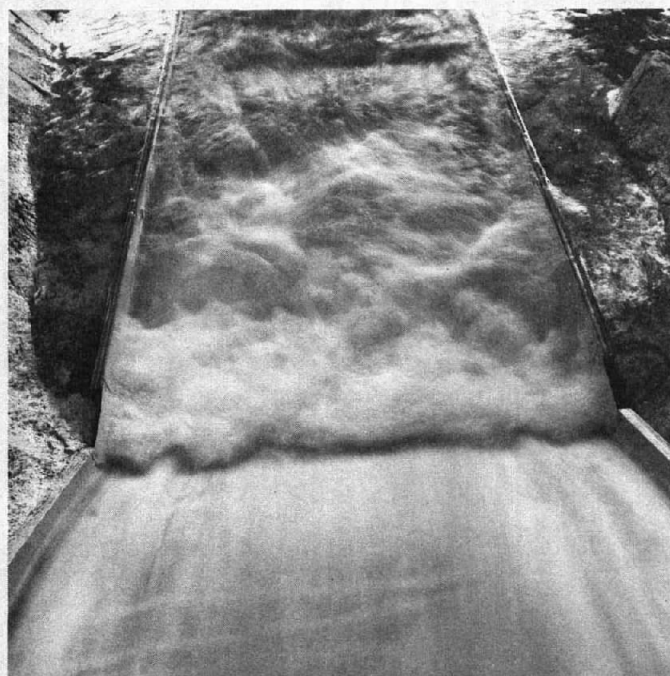


Figure 24.—Spillway stilling basin operation for $Q = 2000 \text{ m}^3/\text{s}$ and tailwater EL 33.4. P801-D-79589.

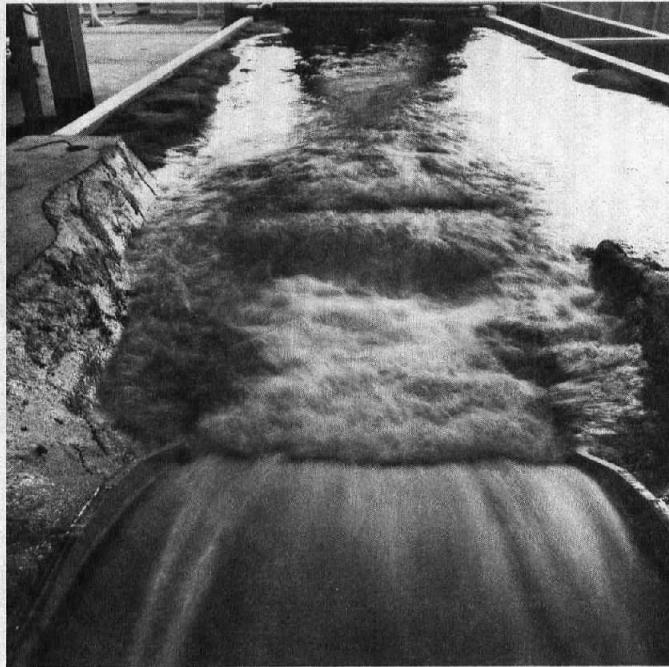


Figure 25.—Spillway stilling basin operation for $Q = 3600 \text{ m}^3/\text{s}$ and tailwater EL 41.5. P801-D-79590.

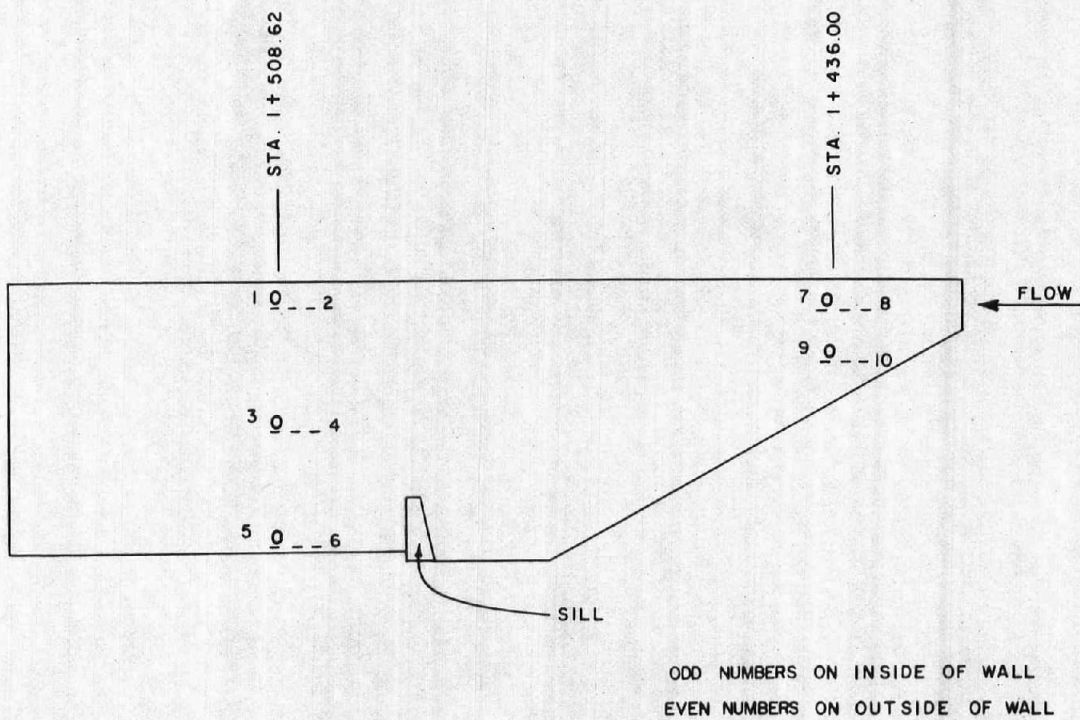


Figure 26.—Piezometer locations along the right wall of the spillway stilling basin.

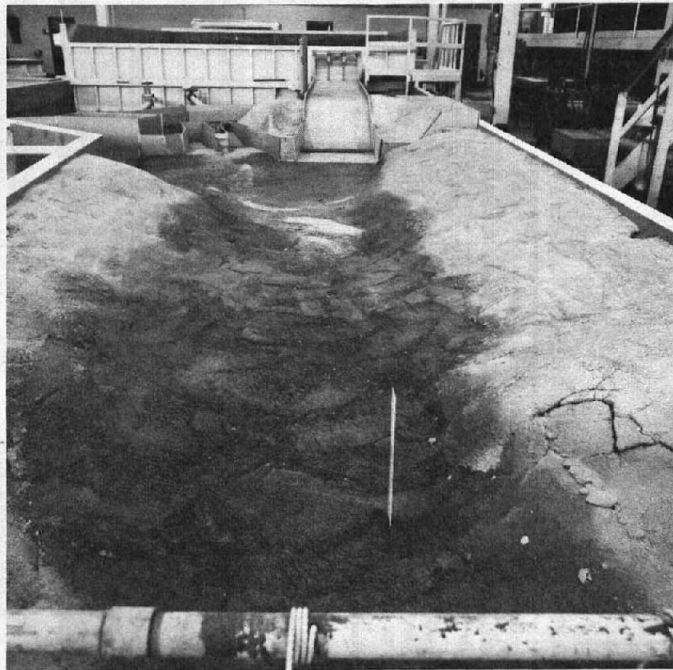


Figure 27.—Stabilized riverbed for spillway model.
P801-D-79591.

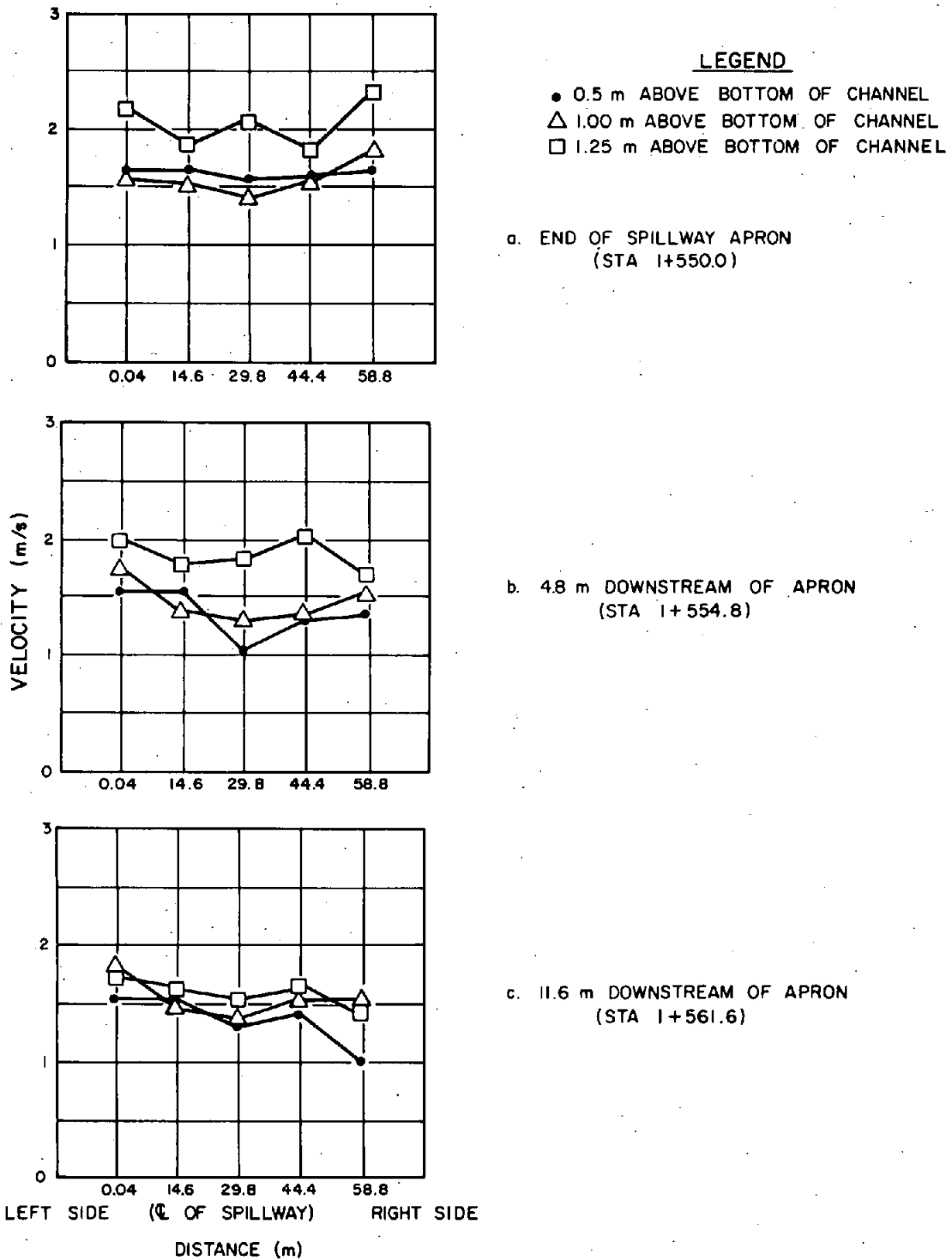
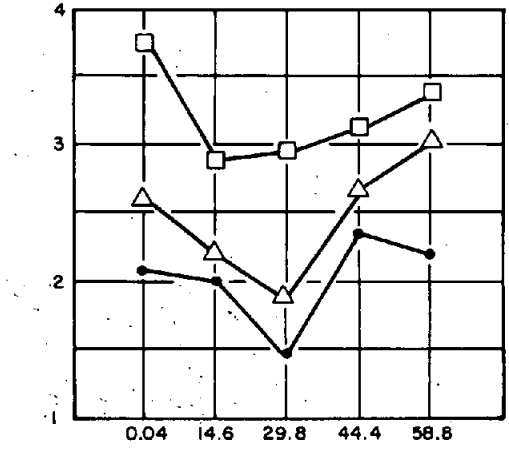


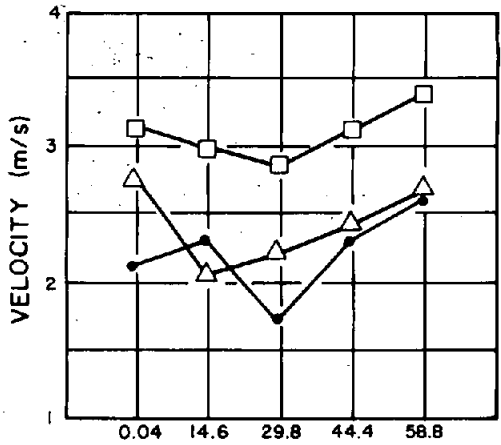
Figure 28.—Graphical representation of the velocities downstream of the spillway stilling basin, $Q = 1000 \text{ m}^3/\text{s}$, tailwater EL 27.



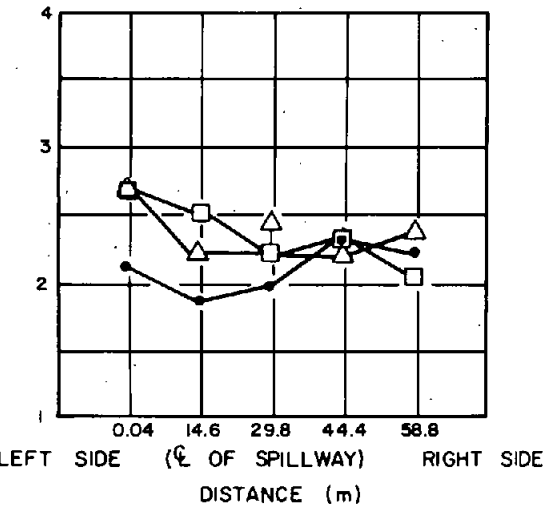
LEGEND

- 0.5 m ABOVE BOTTOM OF CHANNEL
- △ 1.00 m ABOVE BOTTOM OF CHANNEL
- 1.25 m ABOVE BOTTOM OF CHANNEL

a. 2.34 m DOWNSTREAM OF APRON
(STA 1+552.34)

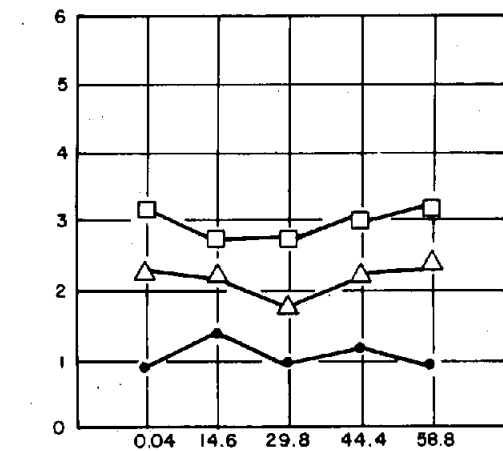


b. 4.0 m DOWNSTREAM OF APRON
(STA 1+554.0)



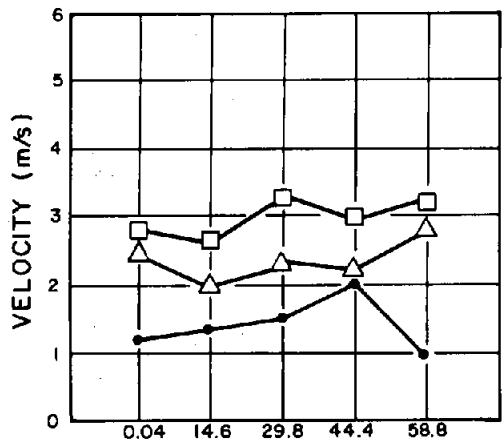
c. 15.6 m DOWNSTREAM OF APRON
(STA 1+565.6)

Figure 29.—Graphical representation of the velocities downstream of the spillway stilling basin, $Q = 1500 \text{ m}^3/\text{s}$, tailwater EL 30.4.

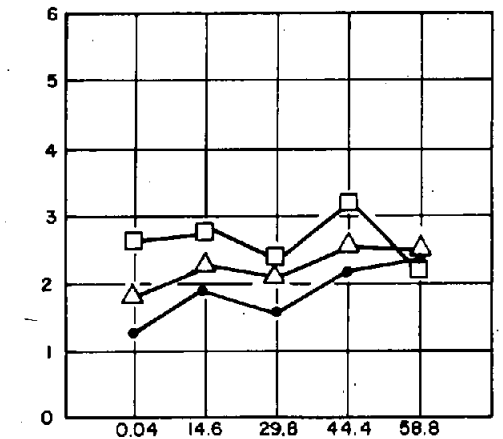


LEGEND
 ● 0.5 m ABOVE BOTTOM OF CHANNEL
 △ 6.3 m ABOVE BOTTOM OF CHANNEL
 □ 12.8 m ABOVE BOTTOM OF CHANNEL

a. 1.1 m DOWNSTREAM OF APRON
(STA 1+551.1)



b. 3.8 m DOWNSTREAM OF APRON
(STA 1+553.8)



c. 14.0 m DOWNSTREAM OF APRON
(STA 1+564.0)

LEFT SIDE (☉ OF SPILLWAY) RIGHT SIDE
 DISTANCE (m)

Figure 30.—Graphical representation of the velocities downstream of the spillway stilling basin, $Q = 2000 \text{ m}^3/\text{s}$, tailwater EL 33.4.

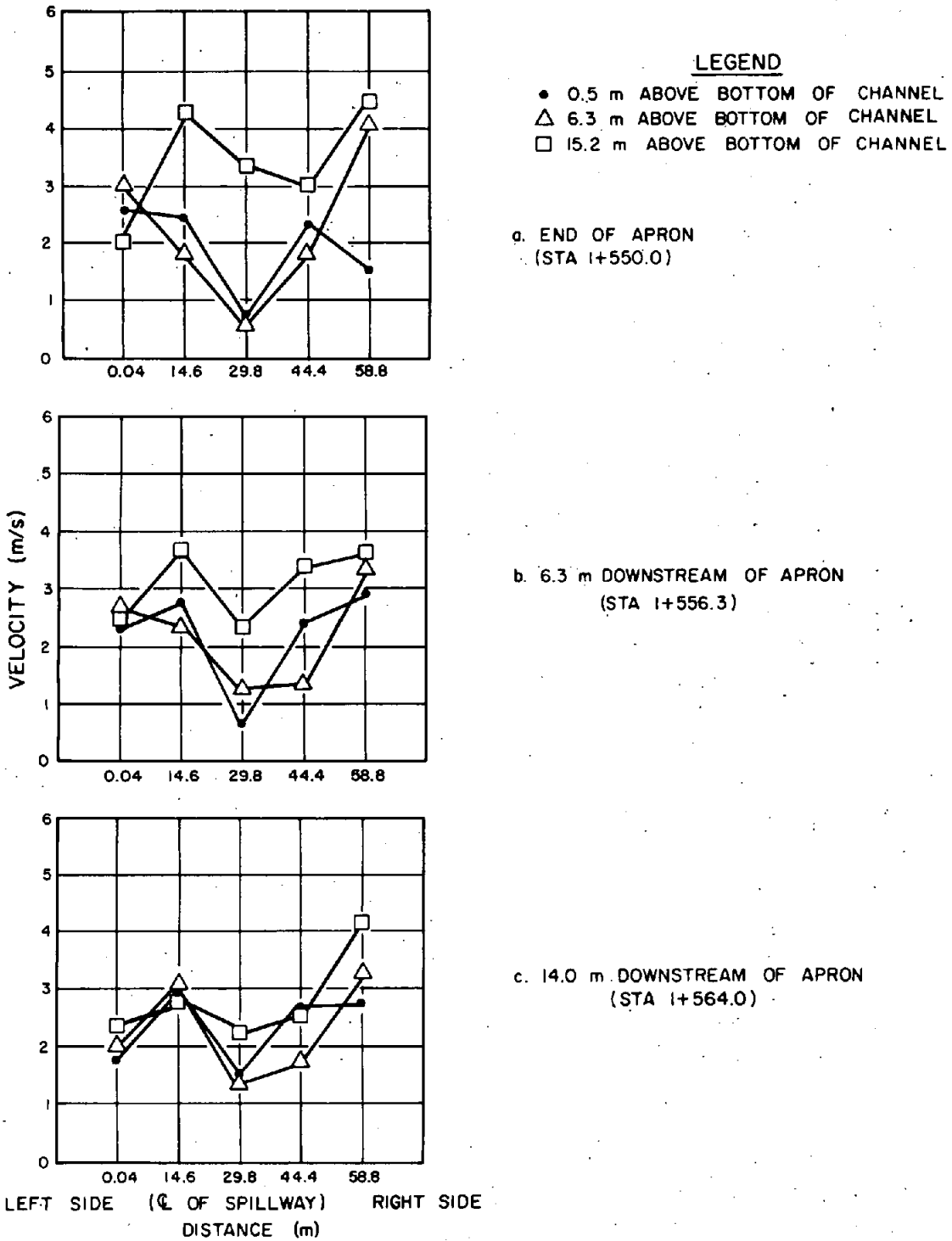


Figure 31.—Graphical representation of the velocities downstream of the spillway stilling basin, $Q = 2500 \text{ m}^3/\text{s}$, tailwater EL 36.2.

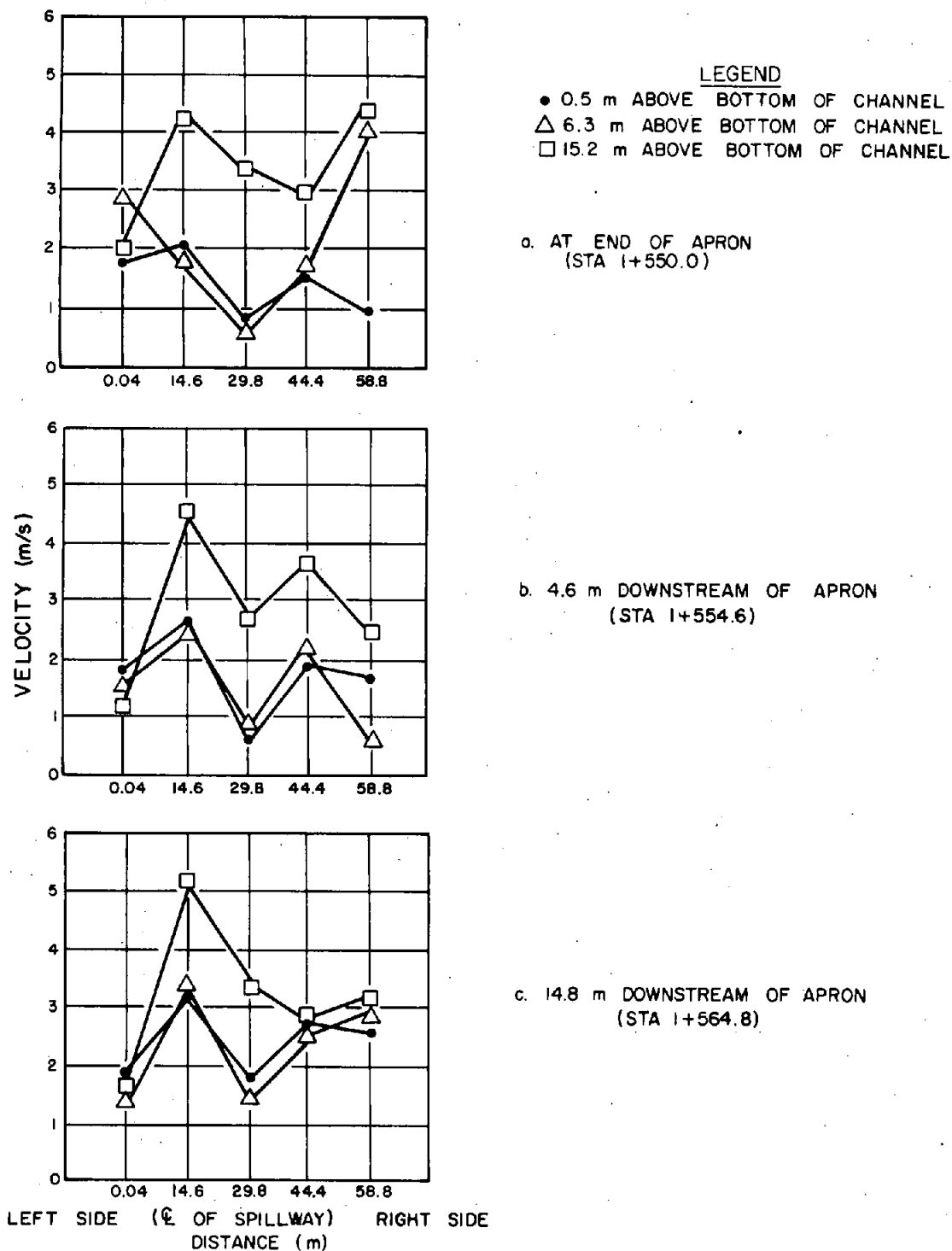
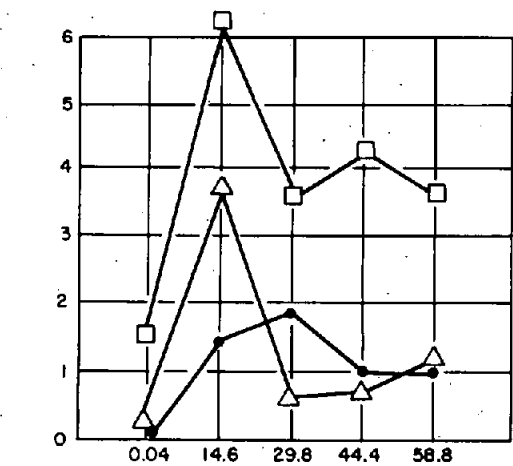
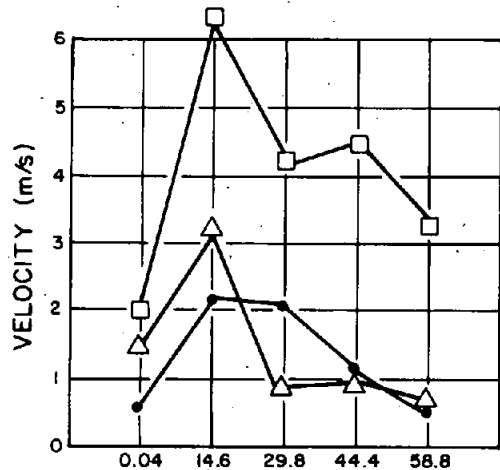


Figure 32.—Graphical representation of the velocities downstream of the spillway stilling basin, $Q = 3000 \text{ m}^3/\text{s}$, tailwater EL 38.7.

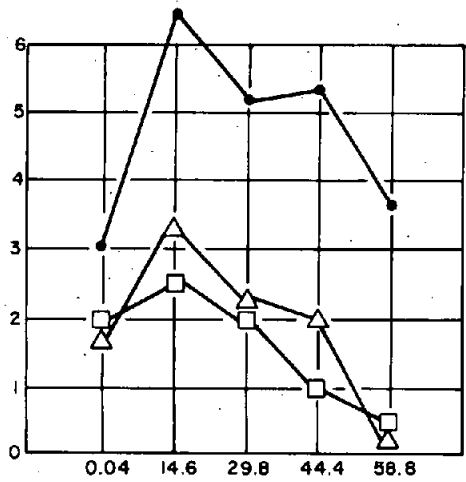


LEGEND
 ● 0.5 m ABOVE BOTTOM OF CHANNEL
 △ 6.3 m ABOVE BOTTOM OF CHANNEL
 □ 15.2 m ABOVE BOTTOM OF CHANNEL

a. 1.0 m DOWNSTREAM OF APRON
(STA 1+551.0)



b. 4.0 m DOWNSTREAM OF APRON
(STA 1+554.0)



c. 14.8 m DOWNSTREAM OF APRON
(STA 1+564.8)

LEFT SIDE (℄ OF SPILLWAY) RIGHT SIDE
 DISTANCE (m)

Figure 33.—Graphical representation of the velocities downstream of the spillway stilling basin, $Q = 3600 \text{ m}^3/\text{s}$, tailwater EL 41.



Figure 34.—Erosion at the toe of the spillway apron and along the left riverbank. P801-D-79592.

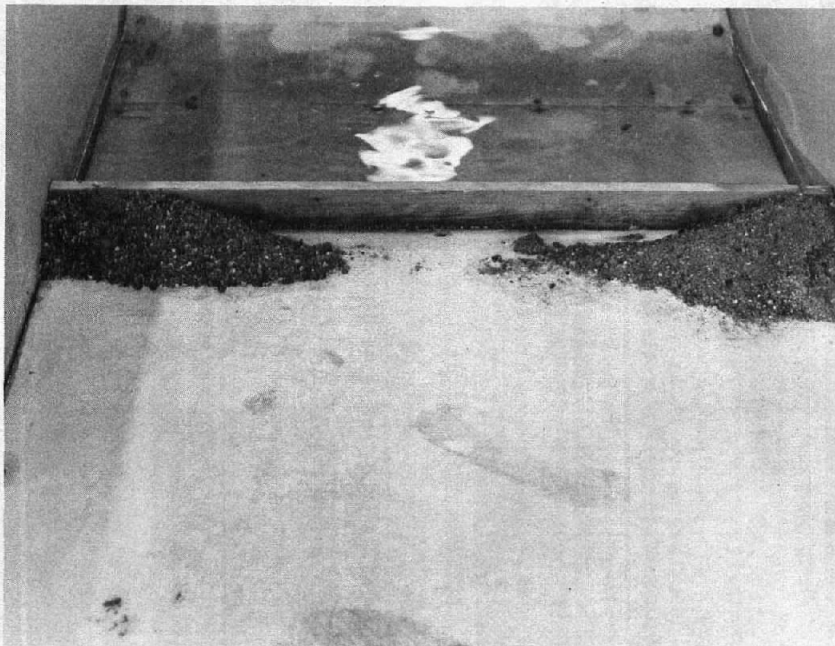


Figure 35.—Deposition of eroded material downstream of the spillway sill. P801-D-79593.



Figure 36.—Eroded material collected behind the left spillway training wall. P801-D-79594.



Figure 37.—Eroded material deposited downstream of the spillway in the river channel at STA 1 + 684.0. P801-D-79595.



Figure 38.—Diversion intake structures, reservoir EL 30, $Q = 593.6 \text{ m}^3/\text{s}$. P801-D-79596.



Figure 39.—Diversion intake structures, reservoir EL 40, $Q = 1472.7 \text{ m}^3/\text{s}$. P801-D-79597.

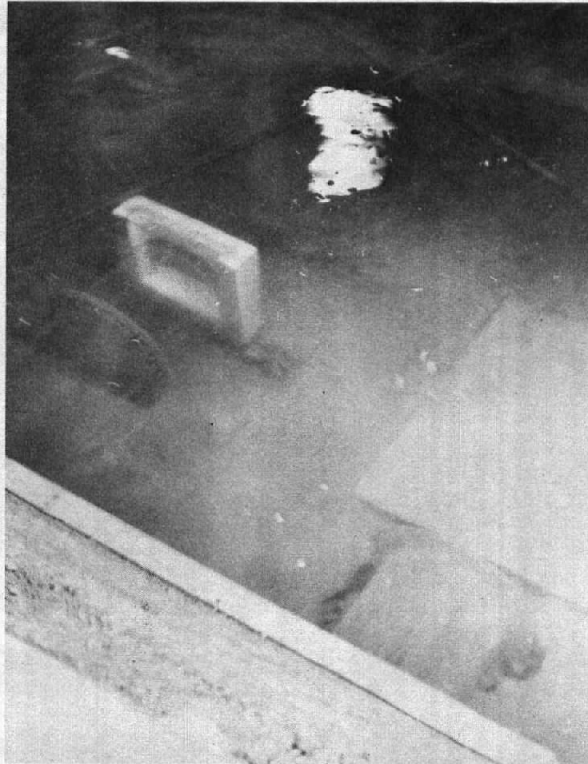


Figure 40.—Diversion intake structures,
reservoir EL 53, $Q = 2007.9 \text{ m}^3/\text{s}$.
P801-D-79598.

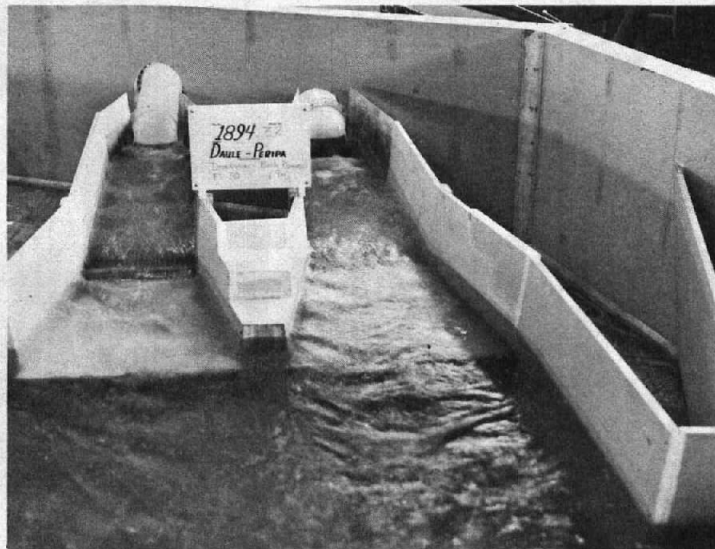


Figure 41.—Diversion stilling basin operation, reservoir EL 30,
 $Q = 593.6 \text{ m}^3/\text{s}$, tailwater EL 23.8. P801-D-79599.

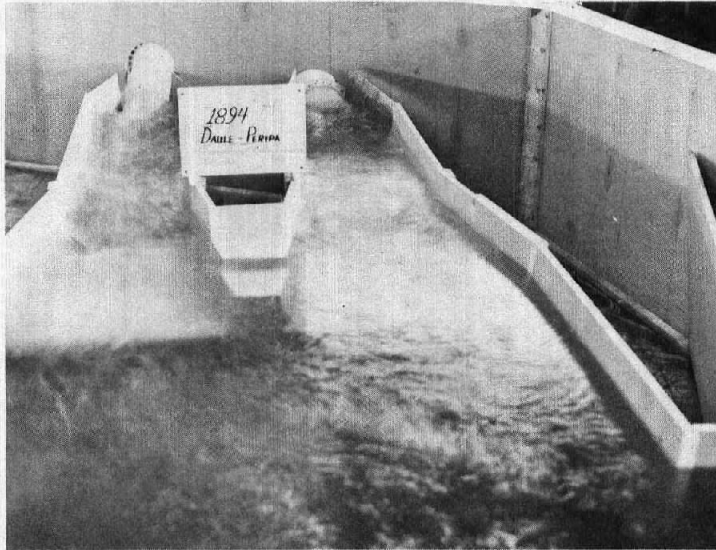


Figure 42.—Diversion stilling basin operation, reservoir EL 40,
 $Q = 1472.7 \text{ m}^3/\text{s}$, tailwater EL 30.3. P801-D-79600.



Figure 43.—Diversion stilling basin operation, reservoir EL 53,
 $Q = 2007.9 \text{ m}^3/\text{s}$, tailwater EL 33.6. P801-D-79601.

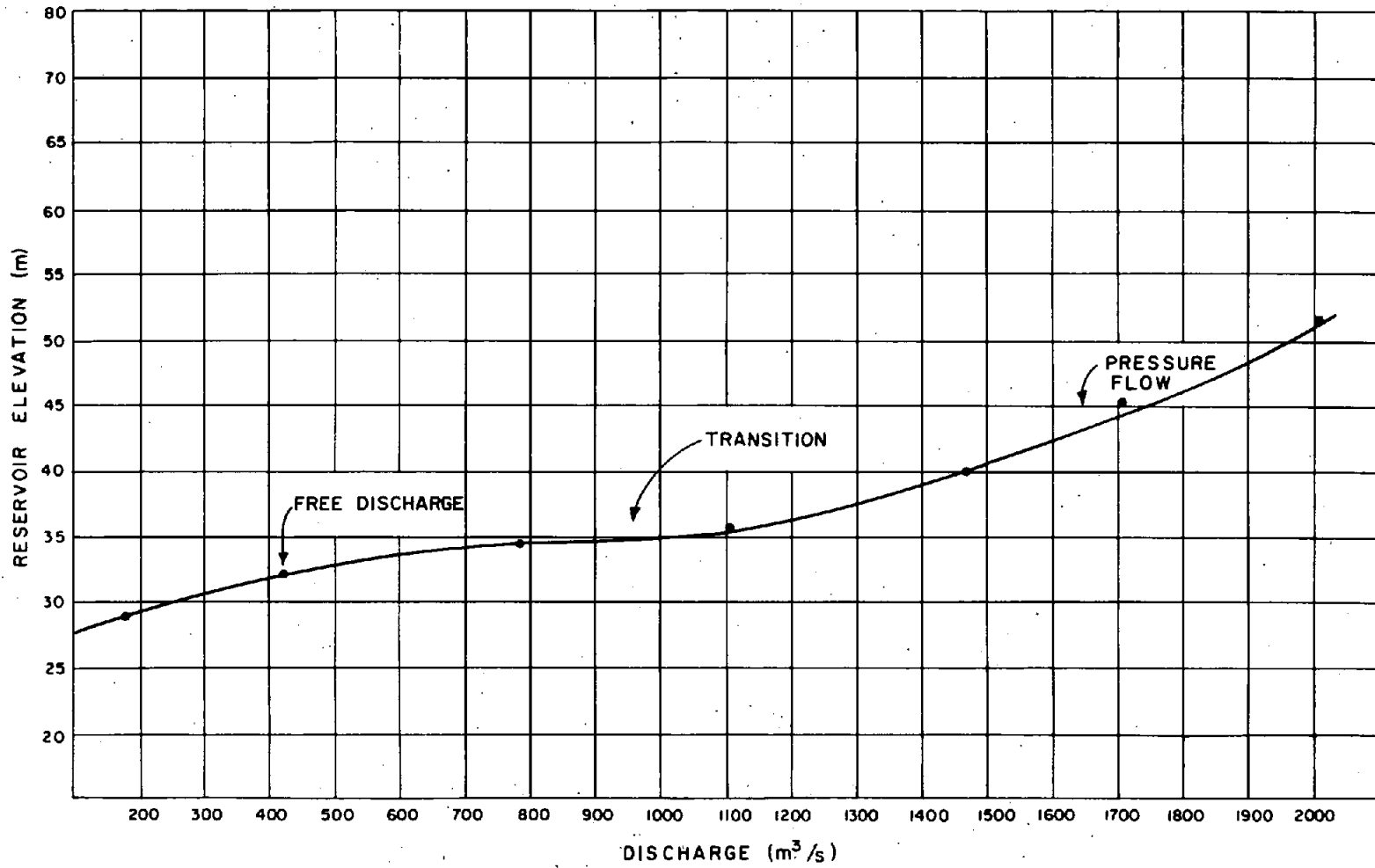


Figure 44.—Diversion discharge curve (both tunnels operating).

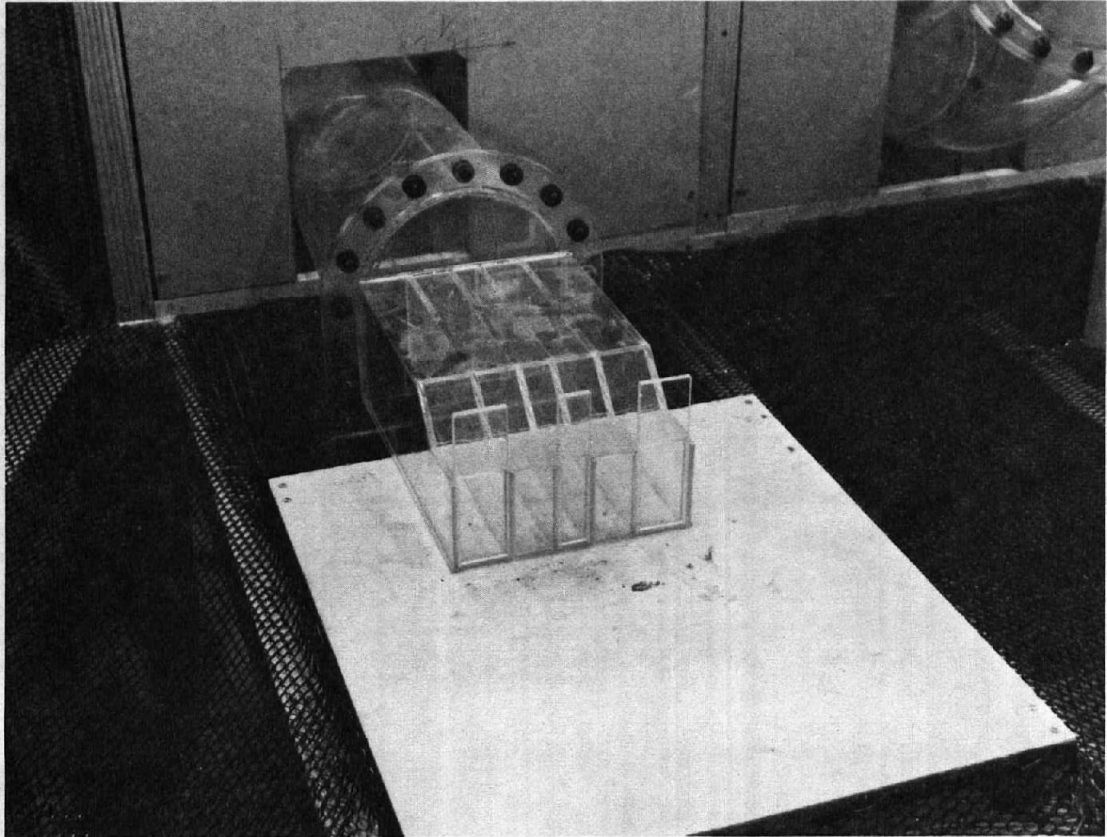


Figure 45.—Modified selective withdrawal tower for the permanent outlet works. P801-D-79602.

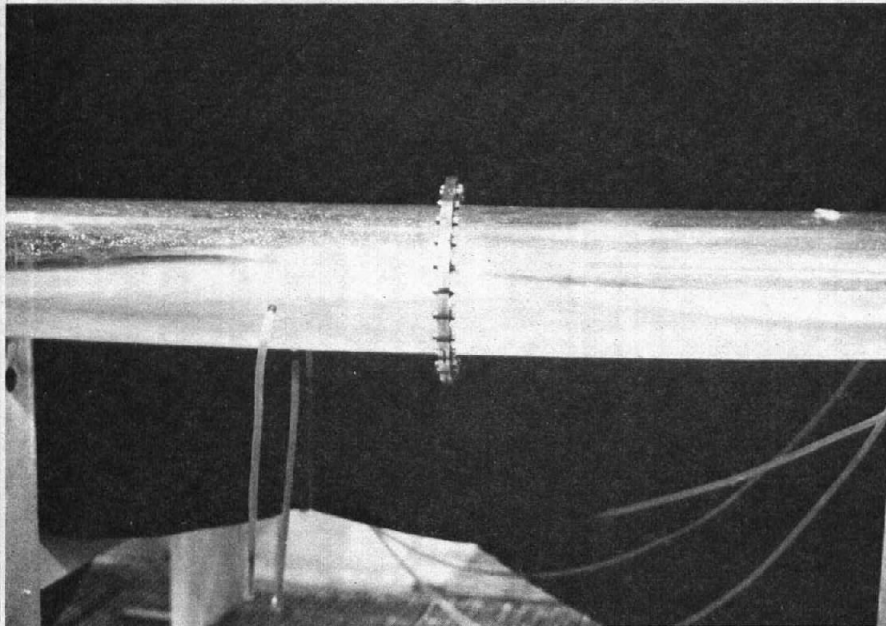


Figure 46.—Tunnel bend with reservoir EL 85, $Q = 422 \text{ m}^3/\text{s}$. P801-D-79603.

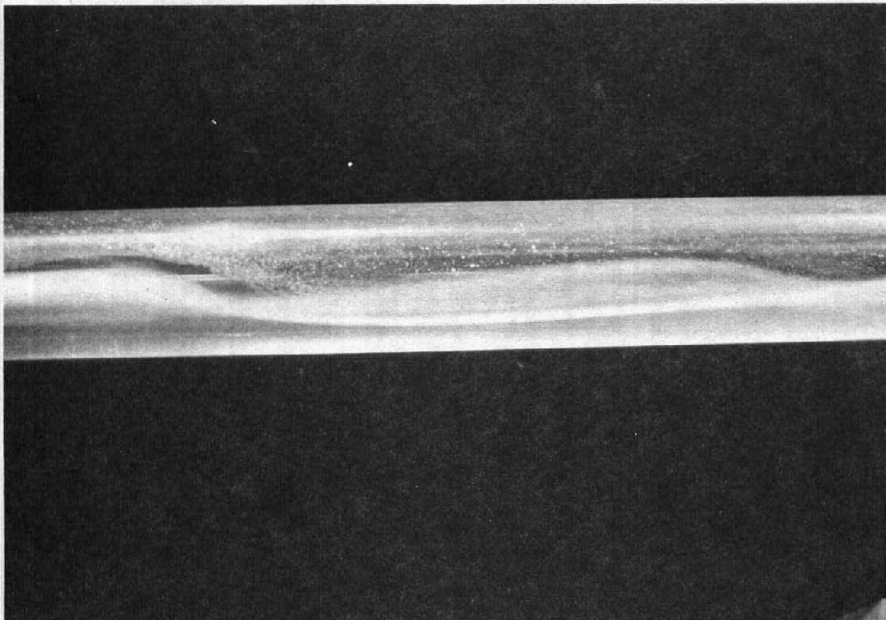


Figure 47.—Oscillating flow downstream of the tunnel bend with reservoir EL 85, $Q = 422 \text{ m}^3/\text{s}$. P801-D-79604.

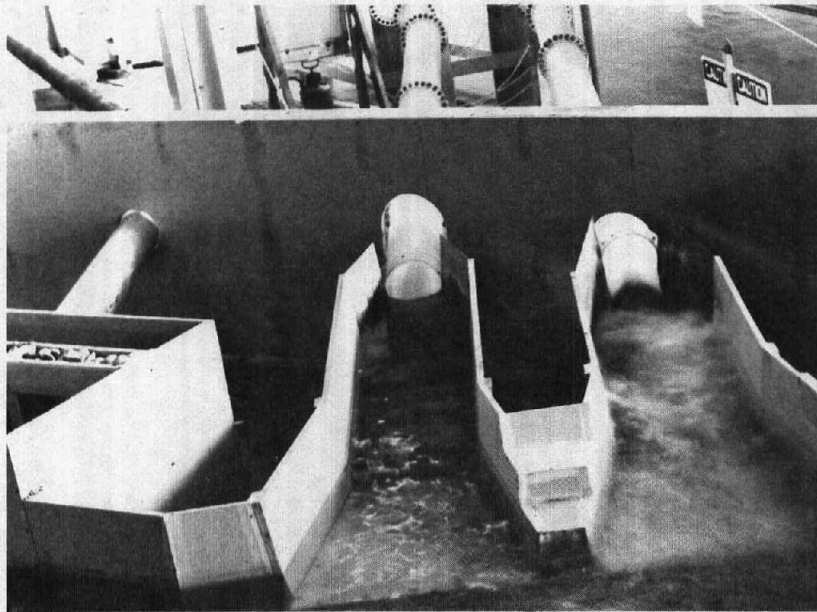


Figure 48.—Stilling basin operation for $Q = 422 \text{ m}^3/\text{s}$ and reservoir EL 85. P801-D-79605.

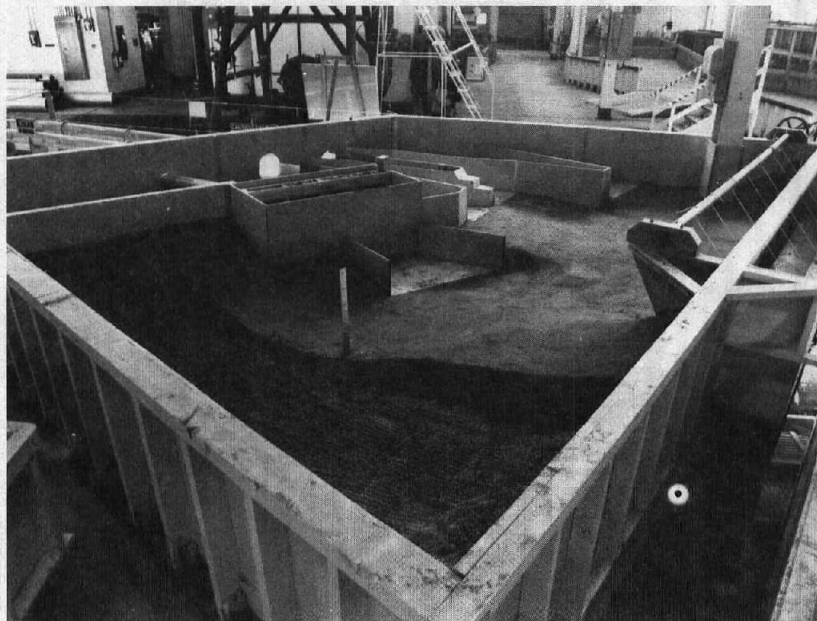
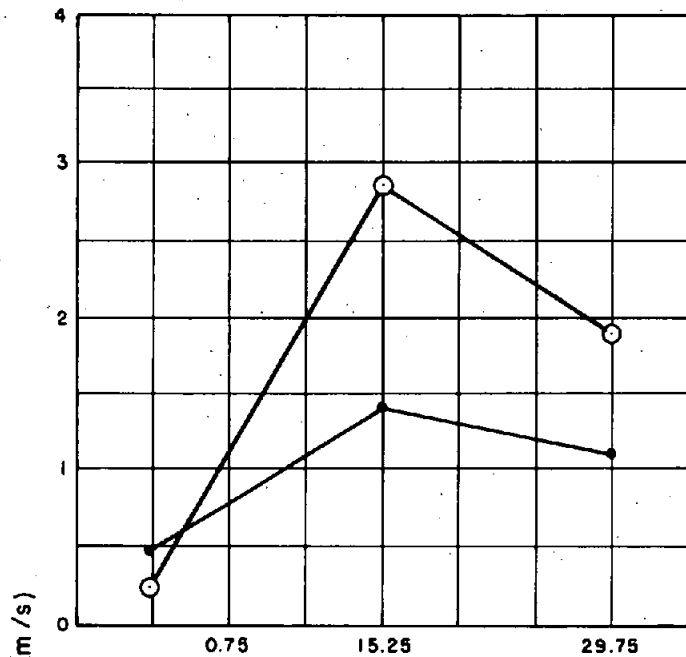
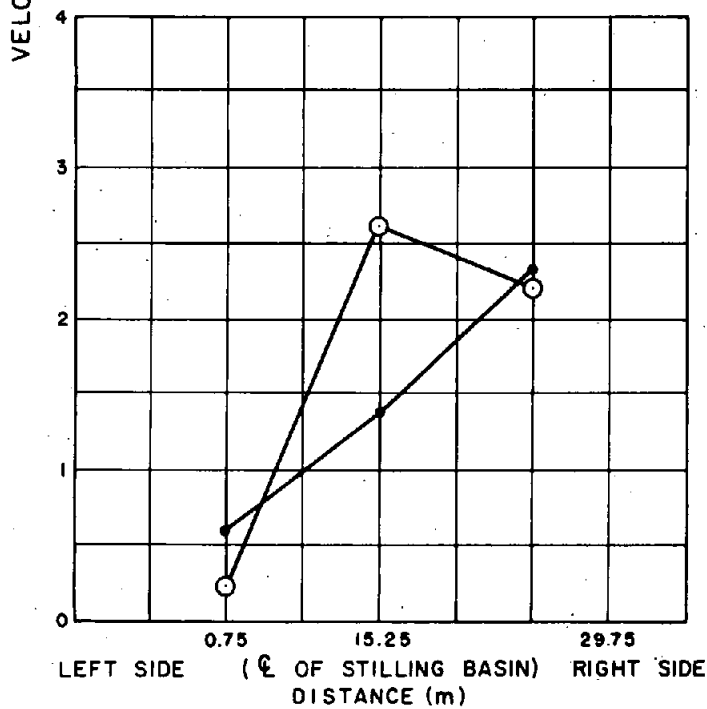


Figure 49.—Stabilized outlet works model riverbed. P801-D-79606.



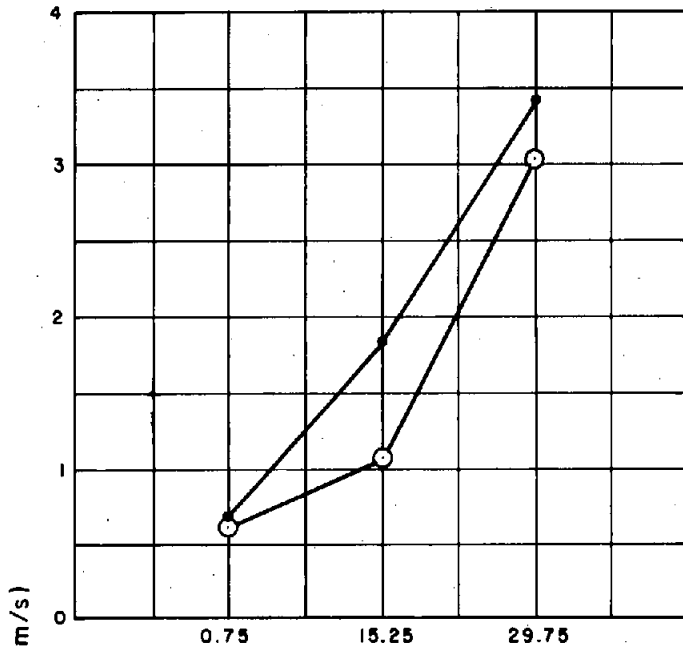
LEGEND
 ● 0.5 m ABOVE BOTTOM OF CHANNEL
 ○ 2.79 m ABOVE BOTTOM OF CHANNEL

a. END OF TUNNEL NO. 1 APRON
 (STA (T-1) 1+ 692.16)



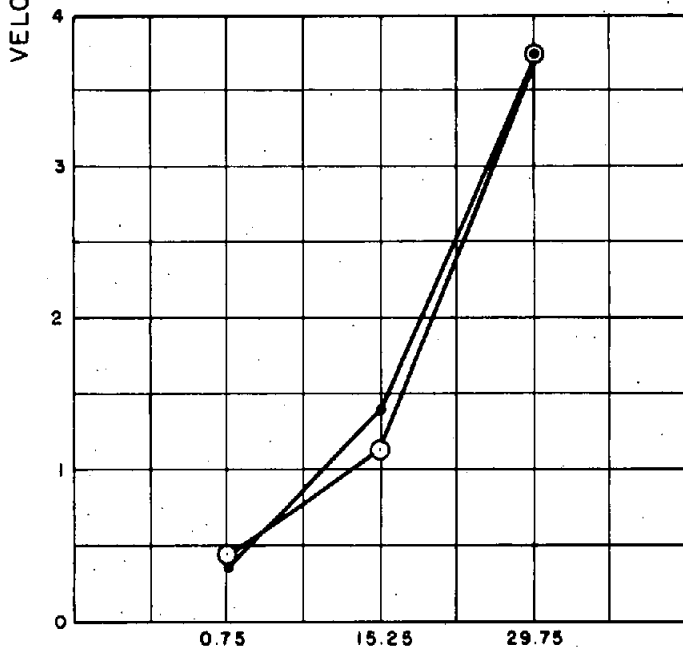
b. 9.64 m DOWNSTREAM OF APRON
 (STA (T-1) 1+701.76)

Figure 50.—Graphical representation of the velocities downstream of the outlet works stilling basin, $Q = 422 \text{ m}^3/\text{s}$, tailwater EL 22.5.



LEGEND
 ● 0.5m ABOVE BOTTOM OF CHANNEL
 ○ 2.79m ABOVE BOTTOM OF CHANNEL

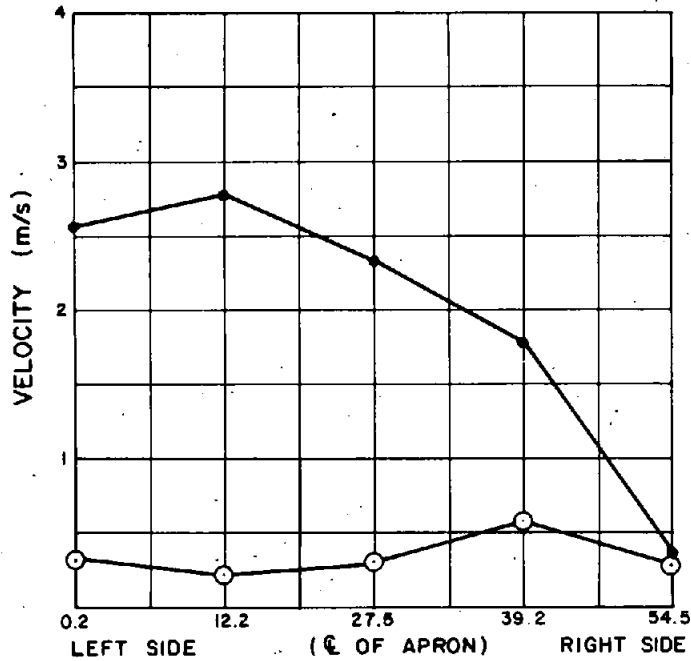
a. END OF TUNNEL NO.1 APRON
 (STA (T-1) 1+692.16)



b. 9.64m DOWNSTREAM OF APRON
 (STA (T-1) 1+701.76)

LEFT SIDE (C OF STILLING BASIN) RIGHT SIDE
 DISTANCE (m)

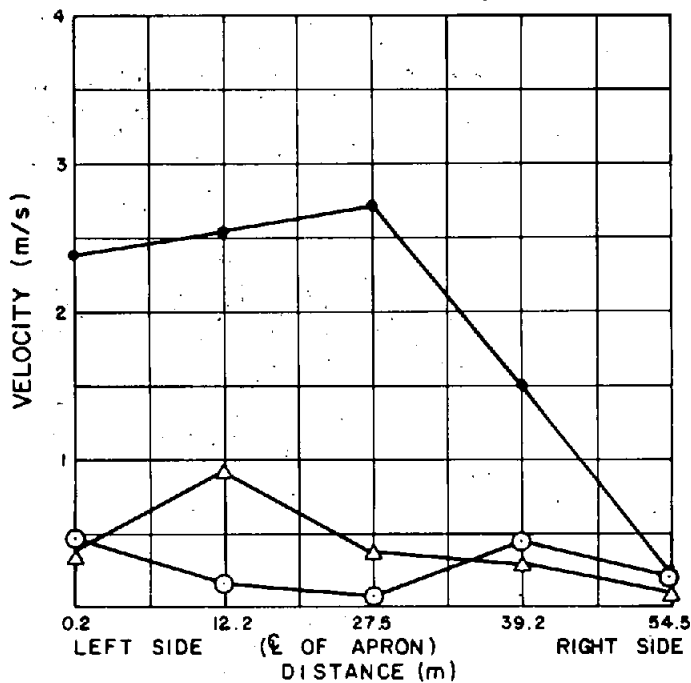
Figure 51.—Graphical representation of the velocities downstream of the outlet works stilling basin, $Q = 672 \text{ m}^3/\text{s}$, tailwater EL 24.6.



LEGEND
 ● 0.5m ABOVE BOTTOM OF CHANNEL
 ○ 2.00m ABOVE BOTTOM OF CHANNEL

END OF POWERPLANT APRON
 (95.5m FROM (T-2) STA 1 + 550
 AT 30° ANGLE)

Figure 52.—Graphical representation of the velocities present downstream for powerplant operation only, $Q = 250 \text{ m}^3/\text{s}$, tailwater EL 20.7.



LEGEND
 ● 0.5m ABOVE BOTTOM OF CHANNEL
 ○ 2.00m ABOVE BOTTOM OF CHANNEL
 △ 4.00m ABOVE BOTTOM OF CHANNEL

END OF POWERPLANT APRON
 (95.5m FROM (T-2) 1 + 550 AT
 30° ANGLE)

Figure 53.—Graphical representation of the velocities present downstream for powerplant and outlet works operation, $Q = 672 \text{ m}^3/\text{s}$, tailwater EL 24.6.

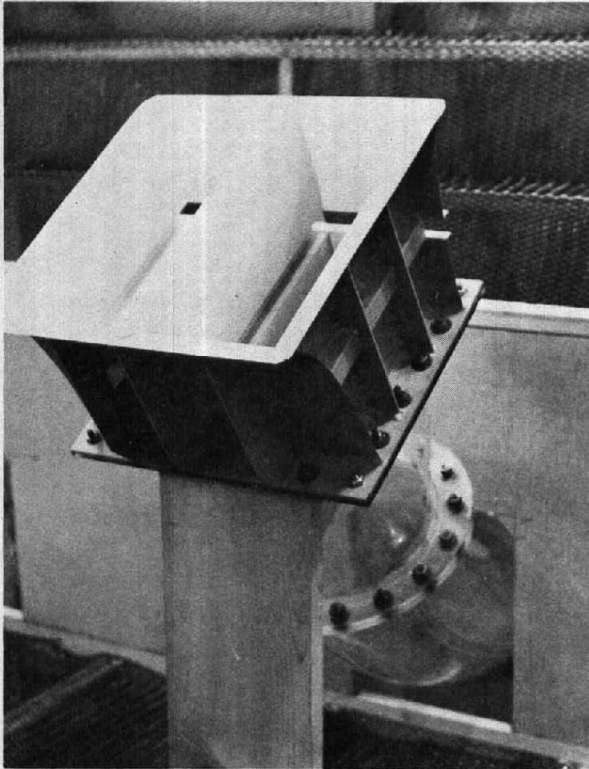


Figure 54.—Bellmouth intake structure.
P801-D-79607.

Figure 55.—Vortex at the bellmouth intake
for reservoir EL 70 without the trashrack.
P801-D-79608.

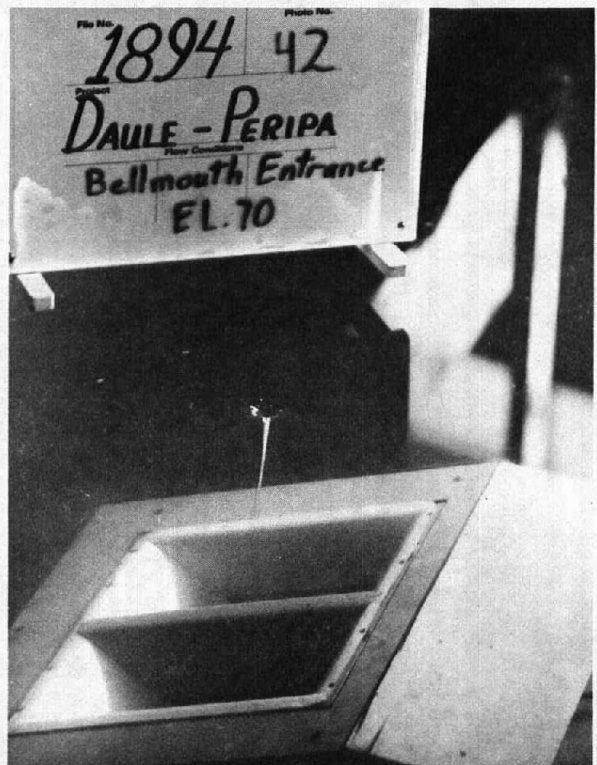




Figure 56.—Vortex at the bellmouth intake for reservoir EL 75 without the trashrack. P801-D-79609.



Figure 57.—Vortex at the bellmouth intake for reservoir EL 80 without the trashrack. P801-D-79610.



Figure 58.—Vortex at the bellmouth intake for reservoir EL 85 without the trashrack. P801-D-79611.

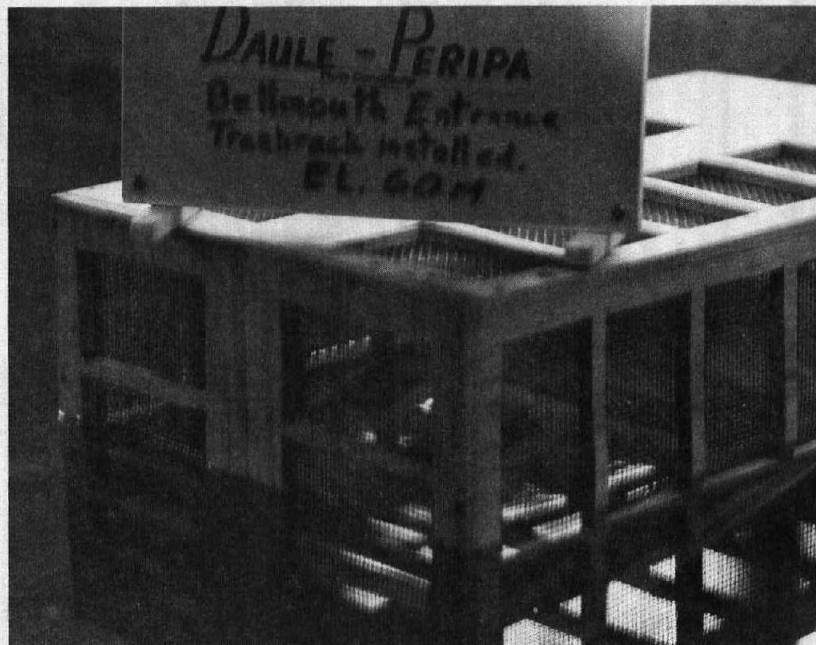


Figure 59.—No vortex formed at reservoir EL 60, $Q = 100 \text{ m}^3/\text{s}$, with the trashrack. P801-D-79612.



Figure 60.—No vortex formed at reservoir EL 75, $Q = 250 \text{ m}^3/\text{s}$, with the trashrack. P801-D-79613.



Figure 61.—No vortex formed at reservoir EL 85, $Q = 250 \text{ m}^3/\text{s}$, with the trashrack. P801-D-79614.

A free pamphlet is available from the Bureau of Reclamation entitled, "Publications for Sale". It describes some of the technical publications currently available, their cost, and how to order them. The pamphlet can be obtained upon request to the Bureau of Reclamation, E&R Center, PO Box 25007, Denver Federal Center, Bldg. 67, Denver, CO 80225, Attn: 922.